INTERNATIONAL ATOMIC ENERGY AGENCY
UNITED NATIONS EDUCATIONAL, SCIENTIFIC AND CULTURAL ORGANIZATION
INTERNATIONAL CENTRE FOR THEORETICAL PHYSICS
I.C.T.P., P.O. BOX 586, 34100 TRIESTE, ITALY, CABLE CENTRATOM TRIESTE

SMR.626 - 20
(lect. III)

The figure you requested contains many pages. We regret there are no better copies available.

SUMMER SCHOOL IN HIGH ENERGY PHYSICS AND COSMOLOGY

15 June - 31 July 1992

RARE DECAYS, MIXING AND CP VIOLATION

AHMED ALI
DESY
Hamburg
Germany

Rare Decays, Mixing, and CP Violation

A. ALI

DESY, Hamburg, FRG

Lecture 3

ICTP, Trieste, July 20, 1992

DESY 92-075
UdeM-LPN-TH95
June 1992

Prospects for Measuring the B_s^0-$\overline{B_s^0}$ Mixing Ratio x_s [1]

A. Ali

Deutsches Elektronen Synchrotron DESY
Hamburg, Germany

D. London

Laboratoire de physique nucléaire, Université de Montréal
C.P. 6128, Montréal, Québec, Canada H3C 3J7

Abstract

We review and update results bearing on the phenomena of particle-antiparticle mixing in the neutral beauty meson sector. Our main focus is on the mixing ratio x_s, defined as $x_s = (\Delta M)/\Gamma$, relevant for B_s^0-$\overline{B_s^0}$ mixing. We present theoretical estimates of this quantity in the standard model and find that $x_s = O(10)$, which makes time-dependent oscillation measurements mandatory. We also discuss estimates of x_s in a number of extensions of the standard model, some of which admit smaller values of x_s. Present and future experimental facilities where such measurements can be undertaken are reviewed on a case to case basis. These include the high luminosity LEP option, asymmetric threshold B-factories, the ep-collider HERA, and hadron colliders, such as the Fermilab Tevatron, LHC and SSC.

[1] Invited article; to be published in Journal of Physics G: Nuclear and Particle Physics, UK.

2 An Update of the CKM Matrix

2.1 The CKM matrix parameters

For 3 generations, the CKM matrix can be described by 3 angles and one complex phase. It was noticed some time ago by Wolfenstein [3] that the elements of this matrix exhibit a hierarchy in terms of λ, the Cabibbo angle. In this parametrisation the CKM matrix can be written approximately as

$$V_{CKM} \simeq \begin{pmatrix} 1-\frac{1}{2}\lambda^2 & \lambda & A\lambda^3(\rho-i\eta) \\ -\lambda & 1-\frac{1}{2}\lambda^2-iA^2\lambda^4\eta & A\lambda^2 \\ A\lambda^3(1-\rho-i\eta) & -A\lambda^2 & 1 \end{pmatrix} \begin{matrix} u \\ c \\ t \end{matrix}$$
$$\begin{matrix} d & s & b \end{matrix}$$

What is known about the four CKM matrix parameters, λ, A, ρ, η? First of all, λ has been extracted with good accuracy from $K \to \pi e \nu$ and hyperon decays [4] to be

$$|V_{us}| = \lambda = 0.2205 \pm 0.0018$$

This agrees quite well with the determination of $V_{us} \simeq 1 - \frac{1}{2}\lambda^2$ from β-decay:

$$|V_{us}| = 0.9744 \pm 0.0010 .$$

Vbc

$B \to D^* \ell \nu_\ell$

$$\lim_{v\cdot v' \to 1} \frac{1}{\sqrt{(v\cdot v')^2-1}} \frac{d\Gamma(B \to D^*(\nu_\ell)}{d(v\cdot v')} = \frac{G_F{}^2}{4\pi^3} M_{D^*}^3 (M_B - M_{D^*})^2 |V_{cb}|^2 \eta_{QCD}^2 \xi(v\cdot v')$$

Parametrization: $\xi(y) = \frac{2}{1+y} exp\{-(2\rho^2-1)\frac{y-1}{y+1}\}$

Isgur-Wise function

$$|V_{cb}| \left(\frac{\tau_{B^0}}{1.18\ ps}\right)^{1/2} = 0.045 \pm 0.007, \quad \rho^2 = 1.19 \pm 0.25.$$

(Neubert)

updated (Schröder): $BR(B \to D^* \ell \nu_\ell) = (5.1 \pm 0.9)\%$

$\tau_B = (1.36 \pm 0.05)$ ps $\Rightarrow |V_{cb}| = 0.046 \pm 0.007$

For the purposes of the fit which follows, we shall use the value of the CKM parameter A obtained from the HQET:

(Marciano)

while the inner corrections are universal. That separation gives rise to a useful nucleus independent quantity

$$Ft = ft(1+\Delta_{inner}) \qquad 12.$$

such that

$$|V_{ud}|^2 = \frac{2884.4 \pm 0.1s}{Ft(1+\Delta_{inner})} \qquad 13.$$

The universal Δ_{inner} has been carefully scrutinized, including a summation of leading short-distance logs, such that (updating ref. 18 for $m_t > 89$ GeV)

$$\Delta_{inner} = 0.0234 \pm 0.0012 \qquad 14.$$

where the error comes primarily from the uncertainty in matching radiative corrections in the effective nucleon theory with short-distance corrections. The estimated error was enhanced by recent calculations (19) of some nuclear structure loop effects that I have included in ft.

Table 2 Ft and $|V_{ud}|$ for various superallowed beta-decays after correcting for nuclear effects, Coulomb, and outer radiative corrections (18). Z represents the charge of the daughter nucleus. The last column includes an empirical correction suggested by fits to the data (20)

Nucleus	Z	Ft (sec)	$\lvert V_{ud}\rvert$	$\lvert V_{ud}\rvert \times (1+(10^{-4}Z)$
^{14}O	7	3067.9 ± 2.4	0.9750 ± 0.0007	0.9756 ± 0.0007
^{26m}AL	12	3071.1 ± 2.6	0.9744 ± 0.0007	0.9756 ± 0.0007
^{34}CL	16	3074.2 ± 3.1	0.9740 ± 0.0008	0.9755 ± 0.0008
^{38m}K	18	3071.5 ± 3.2	0.9744 ± 0.0008	0.9762 ± 0.0008
^{42}Sc	20	3077.1 ± 2.9	0.9735 ± 0.0008	0.9754 ± 0.0008
^{46}V	22	3078.7 ± 3.2	0.9732 ± 0.0008	0.9754 ± 0.0008
^{50}Mn	24	3073.2 ± 5.2	0.9741 ± 0.0010	0.9765 ± 0.0010
^{54}Co	26	3075.1 ± 3.7	0.9738 ± 0.0008	0.9764 ± 0.0008
	Average	3073.0 ± 1.1	0.9741 ± 0.0006	0.9757 ± 0.0006

In Table 2, an up-to-date survey of Ft values is given for various superallowed transitions. If one accepts the small Ft errors, the agreement is not very good. On that basis, it has been argued (20) that nuclear corrections may have introduced a spurious Z dependence in the Ft values. Empirical studies hint at an additional correction that reduces

Schröder (Aachen, June '92)

MODEL INDEPENDENT DETERMINATION

OF $|V_{cb}|$ (NEUBERT)

$BR(B \to D^* \ell \nu) = (5.1 \pm 0.9)\%$

$\tau_B = (1.36 \pm 0.05)\,ps$

$|V_{cb}| = 0.046 \pm 0.007$

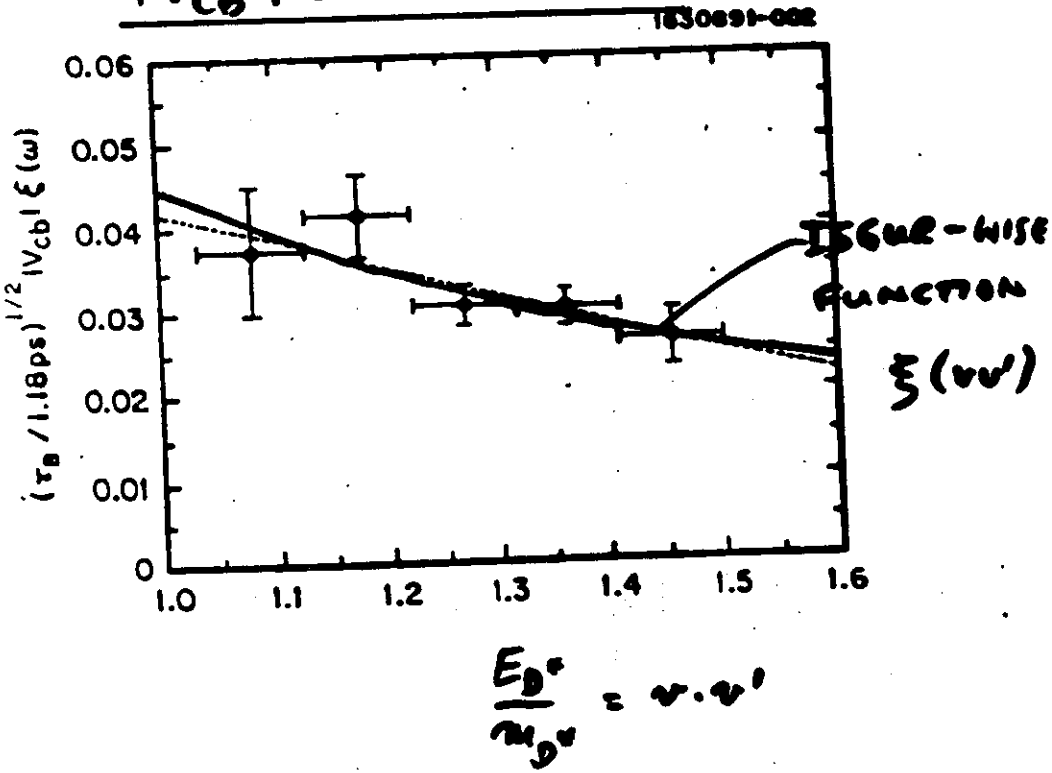

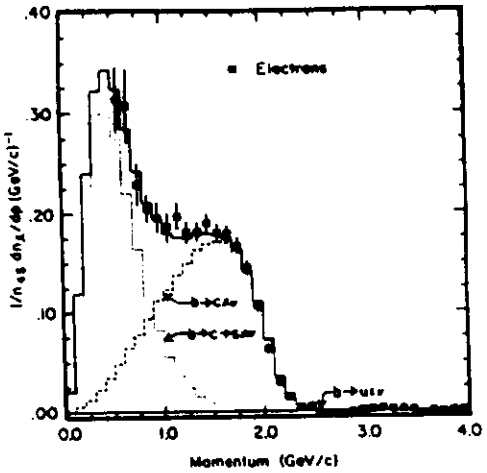

Figure 8: Electron energy spectrum from the Υ(4S) decays by the CLEO collaboration. The fit corresponds to the model of Altarelli et al.

discussion).

Such QCD-improved spectator models have received quite a bit of experimental scrutiny.[68–71] In a recent analysis by the CLEO collaboration, both the electron and muon spectra from the decays $b \longrightarrow c\ell^-\nu_\ell, (\ell = e, \mu)$ have been fit to determine the parameters m_c (equivalently r) and P_F, with the result $P_F = 0.30 \pm 0.09$ GeV and $m_c = 1.680 \pm 0.086$ GeV,[68] with $\frac{\chi^2}{DoF} = \frac{17.4}{31}$. The result of an analysis by the ARGUS collaboration is very similar.[70] The resulting electron energy spectrum from CLEO and the fit to the model of Altarelli et al[55] are shown in Fig. 8. It is fair to conclude, that despite model dependence, which is arguably small, the charged current J_μ^{CC} in b-decays is V-A. Very similar conclusion is reached in the analysis of exclusive decays, in particular $B \longrightarrow D^*\ell\nu_\ell$, where both the vector and axial-vector currents contribute and the shape of the lepton-energy spectrum is likewise sensitive to the chirality of J_μ^{CC}. This test can be put on a more rigorous footing if one could extract the form factors from the decay $B \longrightarrow D^*\ell\nu_\ell$. As an alternative, one could attempt to correct the inclusive lepton energy spectrum for the model dependence, much the same way as it is routinely done in inclusive jet distributions, and then extract the b-quark Michel parameter.

$b \to u l^- \bar{\nu}_l$ (inclusive)

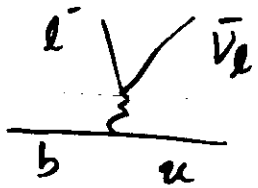

Method	ARGUS data $p_e > 2.3$ GeV	CLEO data $p_e > 2.4$ GeV
ACCMM [5]	0.11 ± 0.01	0.12 ± 0.02
ISGW [6]	0.20 ± 0.02	0.19 ± 0.03
WBS [7]	0.13 ± 0.02	0.13 ± 0.02
KS [8]	0.11 ± 0.01	0.11 ± 0.01

Table 1: Values of V_{ub}/V_{cb} for different theoretical models, from [21].

Recently, the ARGUS collaboration has presented evidence for the exclusive d
$B \to \rho l \nu_l$ [22]. The ratio $|V_{ub}/V_{cb}|$ extracted is quite model-dependent:

$B \to \rho l \nu_l \Rightarrow$ (ARGUS)

$$\left|\frac{V_{ub}}{V_{cb}}\right| = \begin{cases} 0.17 \pm 0.03, & \text{WBS [7]}; \\ 0.30 \pm 0.06, & \text{ISGW [6]}; \\ 0.15 \pm 0.03, & \text{KS [8]}. \end{cases}$$

It is clear that, although there is quite good evidence for a non-zero $|V_{ub}/V_{cb}|$, its value quite uncertain. We shall take (somewhat arbitrarily)

$$\boxed{\left|\frac{V_{ub}}{V_{cb}}\right| = 0.14 \pm 0.05} \tag{24}$$

his gives

$$\boxed{\sqrt{\rho^2 + \eta^2} = 0.63 \pm 0.23} \tag{25}$$

References

[1] S.L. Glashow, Nucl. Phys. 22 (1961) 579; A. Salam in Elementary Particle Theor ed. N. Svartholm (Almqvist and Wiksell, Stockholm, 1968); S. Weinberg, Phys. R Lett. 19 (1967) 1264.

[2] N. Cabibbo, Phys. Rev. Lett. 10 (1963) 531; M. Kobayashi and T. Maskawa, Pr Theor. Phys. 49 (1973) 652.

[3] L. Wolfenstein, Phys. Rev. Lett. 51 (1983) 1945.

[4] M. Aguilar-Benitez et. al. (Particle Data Group), Phys. Lett. B239(1990) 1.

[5] G. Altarelli, M. Cabibbo, G. Corbo, L. Maiani and G. Martinelli, Nucl. Phys. B2 (1982) 365.

[6] N. Isgur, D. Scora, B. Grinstein and M. Wise, Phys. Rev. D39 (1989) 799.

[7] M. Wirbel, B. Stech and M. Bauer, Z. Phys. C29 (1985) 637.

[8] J.G. Körner and G.A. Schuler, Z. Phys. C38 (1988) 511.

[9] N. Isgur and M. Wise, Phys. Lett. B232 (1989) 113; B237 (1990) 527.

[10] M.E. Luke, Phys. Lett. 252B (1990) 447.

[11] C.G. Boyd and D.E. Brahm, Phys. Lett. 257B (1991) 393.

[12] M. Neubert and V. Rieckert, Heidelberg Preprint HD-THEP-91-6 (1991); M. Neube Phys. Lett. 264B (1991) 455, and Heidelberg Preprint HD-THEP-91-30 (1991).

[13] H. Albrecht et. al. (ARGUS Collaboration), Phys. Lett. B229 (1989) 175.

[14] P. Roudeau, Proceedings of the *International Lepton-Photon Symposium and Eu physics Conference on High Eneregy Physics*, S. Hegerty, K. Potter and E. Querci eds. (Geneva, 1991), to appear.

[15] E653 Collaboration (Paper submitted to the *International Lepton-Photon Symposi and Europhysics Conference on High Eneregy Physics*, Geneva, 1991).

[16] R. Fulton et. al. (CLEO Collaboration), Phys. Rev. D43 (1991) 651.

[17] H. Albrecht et. al. (ARGUS Collaboration), DESY 92-029 (1992).

[18] *Heavy Quark Effective Theory*, T. Mannel, Technische Hochschule Darmstadt Rep

CP Violation in the K-System

- $K_L \to 2\pi \implies$ CP-violation
- $K_S \to 3\pi$

$$\boxed{\varepsilon = \frac{A(K_L \to (\pi\pi)_{I=0})}{A(K_S \to (\pi\pi)_{I=0})}}$$

$$A(K^0 \to \pi^+\pi^-) = \sqrt{\tfrac{2}{3}} A_0 e^{i\delta_0} + \sqrt{\tfrac{1}{3}} A_2 e^{i\delta_2}$$

$$A(K^0 \to \pi^0\pi^0) = \sqrt{\tfrac{2}{3}} A_0 e^{i\delta_0} - 2\sqrt{\tfrac{1}{3}} A_2 e^{i\delta_2}$$

$$\Rightarrow \boxed{\varepsilon = \frac{e^{i\pi/4}}{\sqrt{2}\,\Delta M}\left(\mathrm{Im}\, M_{12} + 2\xi\, \mathrm{Re}\, M_{12}\right)}$$

- $2\,\mathrm{Re}\, M_{12} \approx \Delta M = m(K_L) - m(K_S) = 3.5 \times 10^{-15}$ GeV
- $\xi = \mathrm{Im}\, A_0 / \mathrm{Re}\, A_0$
- $\boxed{\varepsilon_{exp} = (2.258 \pm 0.018) \times 10^{-3}\, e^{i\pi/4}}$

Indirect CP violation in $K \to 2\pi$ & ε'/ε

Writing: $K_S = \frac{1}{\sqrt{1+|\bar\varepsilon|^2}}(K_1 + \bar\varepsilon K_2)$ $\overset{CP}{=} |K_1 K_2\rangle$

$K_L = \frac{1}{\sqrt{1+|\bar\varepsilon|^2}}(K_2 + \bar\varepsilon K_1) \overset{CP}{=} \pm |K_1 K_2\rangle$

$K_L \to 2\pi$ via K_1 ($m \propto \bar\varepsilon$ indirect CP)

or $K_L \to K_2 \to \pi\pi$ (direct CP)

- ε'/ε a measure of direct CP

$$\eta_{00} \equiv \frac{A(K_L \to \pi^0\pi^0)}{A(K_S \to \pi^0\pi^0)} \simeq \varepsilon - 2\varepsilon'$$

$$\eta_{+-} \equiv \frac{A(K_L \to \pi^+\pi^-)}{A(K_S \to \pi^+\pi^-)} \simeq \varepsilon + \varepsilon'$$

$$\boxed{|\eta_{00}/\eta_{+-}|^2 \simeq 1 - 6\,\mathrm{Re}(\varepsilon'/\varepsilon)}$$

$\Rightarrow$ Exptl. ratio (E731, NA31)

Th: $\boxed{\frac{\varepsilon'}{\varepsilon} = -\frac{\omega}{\sqrt{2}}\frac{1}{|\varepsilon|}\frac{\mathrm{Im}\, A_0}{\mathrm{Re}\, A_0}\left[1 - \frac{1}{\omega}\frac{\mathrm{Im}\, A_2}{\mathrm{Im}\, A_0}\right]}$

- Phases: $\phi(\varepsilon') = (45 \pm 6)^\circ$, $\phi(\varepsilon) = \pi/4$ $\Rightarrow \boxed{\phi(\varepsilon - \varepsilon') \simeq 0}$

$\omega \simeq 1/20$

$\Rightarrow \varepsilon'/\varepsilon \simeq \mathrm{Re}(\varepsilon'/\varepsilon) = (23 \pm 7) \times 10^{-4}$ NA31

(Buras et al.)

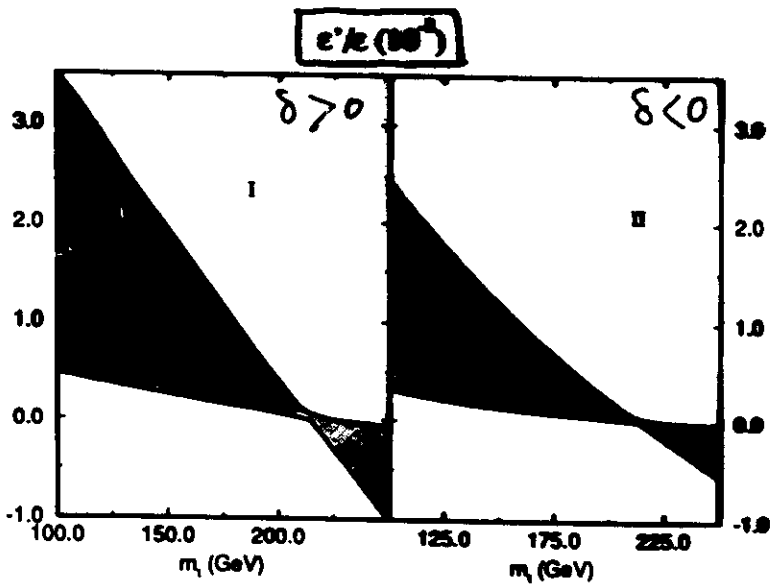

Fig. 2: The upper and lower limits of ε'/ε in the first (I) and second (II) quadrant of δ, respectively. The following parameter ranges have been used: $0.09 \le |V_{cb}|/|V_{cb}| \le 0.17$, $0.036 \le |V_{cb}| \le 0.046$, 0.1 GeV $\le \Lambda_{QCD} \le 0.3$ GeV, $0.5 \le B_K \le 0.8$ and 125 MeV $\le m_s \le 200$ MeV.

⇒ $\mathrm{Re}\,\varepsilon'/\varepsilon \simeq \varepsilon'/\varepsilon$ in SM depends on m_t + $\sin\delta$ (δ = KM phase)

- depending on m_t, SM compatible with both E731 and NA31 !
- no useful constraints on SM parameters

The experimental value of $|\epsilon|$ is

$$|\epsilon| = (2.26 \pm 0.02) \times 10^{-3}$$

Theoretically, $|\epsilon|$ is essentially proportional to the imaginary part of the box diagram for K^0-$\overline{K^0}$ **mixing** (Fig. 1), and is given by [23]

$$|\epsilon| = \frac{G_F^2 f_K^2 M_K M_W^2}{6\sqrt{2}\pi^2 \Delta M_K} B_K \left(A^2\lambda^6\eta\right)\left(y_c\left\{\eta_{ct} f_3(y_c, y_t) - \eta_{cc}\right\} + \eta_{tt} y_t f_2(y_t) A^2\lambda^4(1-\rho)\right).$$

Here, the η_i **are QCD correction factors,** $\eta_{cc} \simeq 0.82$, $\eta_{tt} \simeq 0.62$, $\eta_{ct} \simeq 0.35$ for $\Lambda_{QCD} = 200$ **MeV** [24], $y_i \equiv m_i^2/M_W^2$, **and the functions** f_2 **and** f_3 **are given by**

$$f_2(x) = \frac{1}{4} + \frac{9}{4}\frac{1}{(1-x)} - \frac{3}{2}\frac{1}{(1-x)^2} - \frac{3}{2}\frac{x^2 \ln x}{(1-x)^3},$$

$$f_3(x,y) = \ln\frac{y}{x} - \frac{3y}{4(1-y)}\left(1 + \frac{y}{1-y}\ln y\right).$$

(The above form for $f_3(x,y)$ **is an approximation, obtained in the limit** $x \ll y$. **For the exact expression, see ref. [25].)**

One of the unknowns in Eq. 27 is the top quark mass. The most model-independent lower bound comes from LEP [26],

$$m_t > 45 \text{ GeV}.$$

There is a stronger lower limit (95% c.l.) of

$$m_t > 89 \text{ GeV}$$

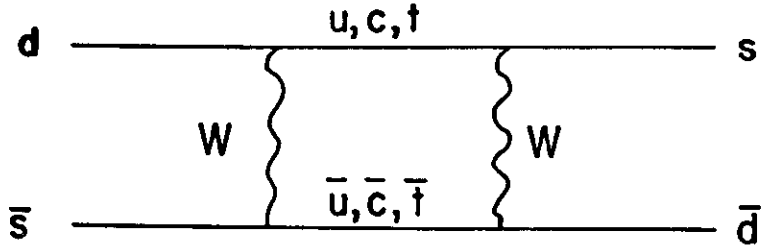

Figure 1: Box diagram for K^0-$\overline{K^0}$ **mixing. There is another diagram in which the internal quark and W lines are interchanged.**

Method	Value of B_K
Vacuum Insertion	1
Hadronic Sum Rules	0.33 ± 0.09 [31]
	0.30 ± 0.10 [32]
Chiral Symmetry	0.33 ± 0.2 [33]
QCD Sum Rules	0.50 ± 0.22 [34]
	0.58 ± 0.16 [35]
	0.84 ± 0.08 [36]
	0.74 ± 0.17 [37]
1/N	0.66 ± 0.10 [38]
Lattice Theories	0.87 ± 0.20 [39]
	1.03 ± 0.07 [40]
	0.94 ± 0.01 [41]
	0.77 ± 0.07 [41]
	0.92 ± 0.03 [42]

Table 2: Values of B_K using different methods of calculation.

used in the analysis: $B_K = 0.8 \pm 0.2$

We now turn to B_d^0-$\overline{B_d^0}$ mixing. The latest value of x_d, which is a measure of this mixing, is [43]

$$x_d = 0.67 \pm 0.10$$

The mixing parameter x_d is calculated from the B_d^0-$\overline{B_d^0}$ box diagram (Fig. 2). Unlike the K^0-$\overline{K^0}$ system, where the contributions of both the c- and the t-quarks in the loop were important, this diagram is dominated by t-quark exchange:

$$x_d \equiv \frac{(\Delta M)_B}{\Gamma} = \tau_B \frac{G_F^2}{6\pi^2} M_W^2 M_B \left(f_{B_d}^2 B_{B_d}\right) \eta_B S(y) f_3(y) |V_{td}^* V_{tb}|^2$$

coupling Constant

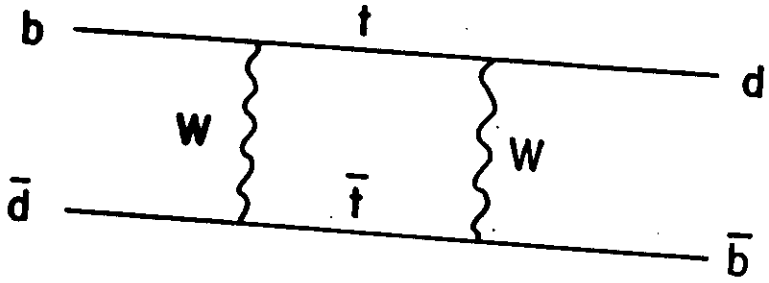

Figure 2: Box diagram for B_d^0-$\overline{B_d^0}$ mixing. There is another diagram in which the internal quark and W lines are interchanged.

$B_d^0 - \overline{B}_d^0$ Mixing

Method	
QCD Sum Rules	$f_{B_s} = 115 \pm 15$ MeV [45] $f_{B_s} = 120 \pm 13$ MeV [46] $f_{B_s} = 170 \pm 20$ MeV [47] $f_{B_s} = 100$-126 MeV [48] $f_{B_s}\sqrt{B_{B_s}} = 185 \pm 25$ MeV [49] $f_{B_s}\sqrt{B_{B_s}} = 150 \pm 30$ MeV [50]
Potential Models Lattice Theories (1)	$f_{B_s} = 155 \pm 15$ MeV [51] $f_{B_s} \sim 120$ MeV [52] $f_{B_s} = 165 \pm 17 \pm 30$ MeV [53]
Lattice Theories (2)	$f_{B_s} = 310 \pm 25 \pm 50$ MeV* [54] $f_{B_s} = 320 \pm 20$ MeV* [55] $f_{B_s} = 188$-246 MeV [56]

Table 3: Values of f_{B_s} and $f_{B_s}\sqrt{B_{B_s}}$ using different methods of calculation. For the entries marked with a *, which have been calculated in the static limit, it is estimated that the $1/m_b$ corrections will reduce these values by about 25% [54].

Method	
Potential Models Lattice Theories (1) (old)	$f_{B_s} = 210 \pm 20$ MeV [51] $f_{B_s} \sim 150$ MeV [52] $f_{B_s} = 155 \pm 31 \pm 48$ MeV [53]
Lattice Theories (2) (New)	$f_{B_s} = 204$-241 MeV [56]

Table 4: Values of f_{B_s} using different methods of calculation.

However, recent lattice calculations do not seem to support the hypothesis that f_{B_s} significantly larger than f_{B_d}: ref. [56] gives

$$f_{B_d} = 188\text{-}246 \text{ MeV}, \qquad f_{B_s} = 204\text{-}241 \text{ MeV}.$$

← Modern Lattice Values

Along the same lines, Abada et al. [57] quote $f_{B_s}/f_{B_d} = 1.06 \pm 0.04$ a recent average of a number of lattice calculations gives $f_{B_s}/f_{B_d} = 1.08 \pm 0.06$ [58].

[45] M.A. Shifman and M.B. Voloshin, ITEP Report ITEP-54 (1986).

[46] S. Narison, Phys. Lett. **B198** (1987) 104.

[47] L.J. Reinders, Phys. Rev. **D38** (1988) 947.

[48] C.A. Dominguez and N. Paver, Phys. Lett. **B269** (1991) 169.

[49] L.J. Reinders and S. Yazaki, Phys. Lett. **B212** (1988) 245.

[50] A. Pich, Phys. Lett. **B206** (1988) 322.

[51] S. Capstick and S. Godfrey, Phys. Rev. **D41** (1990) 2856.

[52] M.B. Gavela et. al., Phys. Lett. **B206** (1988) 113.

[53] C. Bernard, T. Draper, G. Hockney and A. Soni, Phys. Rev. **D38** (1988) 3540.

[54] C.R. Allton et. al., Nucl. Phys. **B349** (1991) 598.

[55] C.W. Bernard, A.X. El-Khadra and A. Soni, presented at the Symposium Lattice '9 Tallahassee, October, 1990.

[56] C. Alexandrou et. al., CERN preprint CERN-TH.6113/91 (1991). *

[57] A. Abada et al., Rome preprint Rome-823-1991 (1991). *

[58] C. Sachrajda, invited talk at the Conference QCD-20 Years Later, Aachen, (Ju 9-13 (1992).

* New Lattice Calculations: [56], [57], [

CKM

The unitarity triangle

The information regarding the allowed region in ρ-η space can be displayed quite elegantly using the so-called unitarity triangle. This is constructed as follows. Because the CKM matrix is unitary, one has the following relation:

$$V_{ub}V_{ud}^{*} + V_{cb}V_{cd}^{*} + V_{tb}V_{td}^{*} = 0$$

Using the form of the CKM matrix in Eq. 1, this can be recast as

$$\frac{V_{ub}^{*}}{\lambda V_{cb}} + \frac{V_{td}}{\lambda V_{cb}} = 1$$

that is, a triangle relation in the complex plane (i.e. ρ-η space). This is illustrated in Fig. 3. Thus, allowed values of ρ and η translate into allowed shapes of the unitarity triangle.

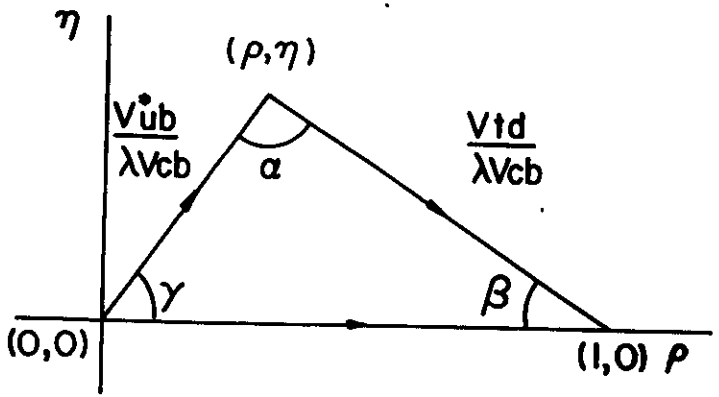

Figure 3: The unitarity triangle. The angles α, β and γ can be measured via CP violation in the B system.

CP

$B_d^{\circ} \to J/\psi K_S \Longrightarrow \sin 2\beta$

$B_d^{\circ} \to \pi^+\pi^- \Longrightarrow \sin 2\alpha$

$B^{\circ} \to \rho K_s \Longrightarrow \sin 2\gamma$

CP in B Decay Amplitudes

Favorite Paradigm: $B_d^{\circ} \to J/\psi K_S$

- involves $B - \bar{B}$ Mixing

$B^{\circ} \to B^{\circ} \to f$

$B^{\circ} \to \bar{B}^{\circ} \to f$

- f a CP Eigenstate

$$\Gamma(\bar{B}^{\circ}(t) \to f) \sim e^{-\Gamma t}\left(1 - \sin(\Delta m t) \cdot \mathrm{Im}\left(\frac{p}{q}\rho\right)\right)$$

$$\Gamma(B^{\circ}(t) \to f) \sim e^{-\Gamma t}\left(1 + \sin(\Delta m t) \cdot \mathrm{Im}\left(\frac{p}{q}\rho\right)\right)$$

with $\rho = \dfrac{A(B \to f)}{A(\bar{B} \to f)} = 1$ for f a CP Eigenstate

$$p/q = \frac{1+\epsilon_B}{1-\epsilon_B}$$

$$A_{CP} = \frac{\Gamma(B) - \Gamma(\bar{B})}{\Gamma(B) + \Gamma(\bar{B})} = \sin(\Delta m t)\, \mathrm{Im}\left(\frac{p}{q}\rho\right)$$

$B = \boxed{\phi = \text{Angle of Unit. } \Delta}$ $\quad T_{\text{dec}}^{III} e^{2i\phi}$

(Dunietz)

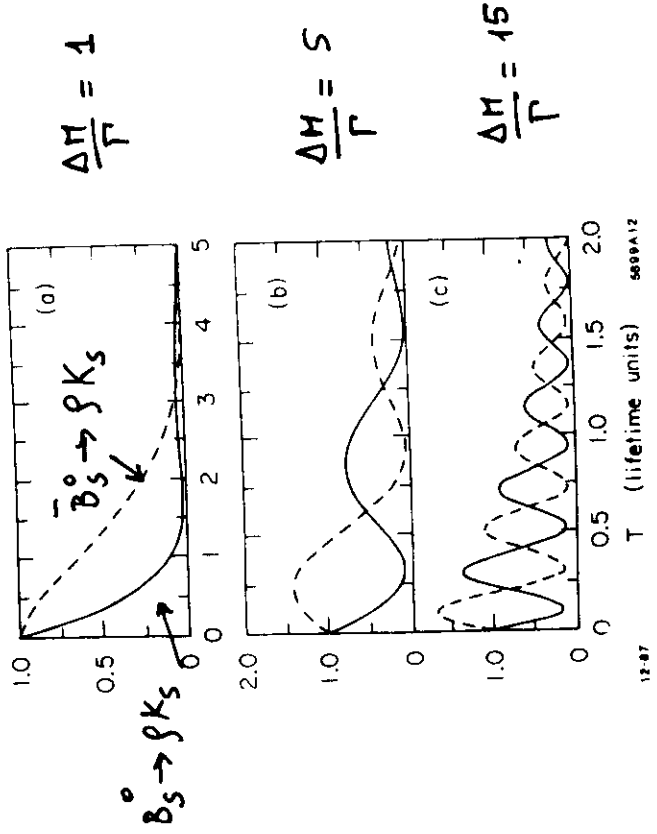

Fig. 13

present status of ΔCKM (London, A·A

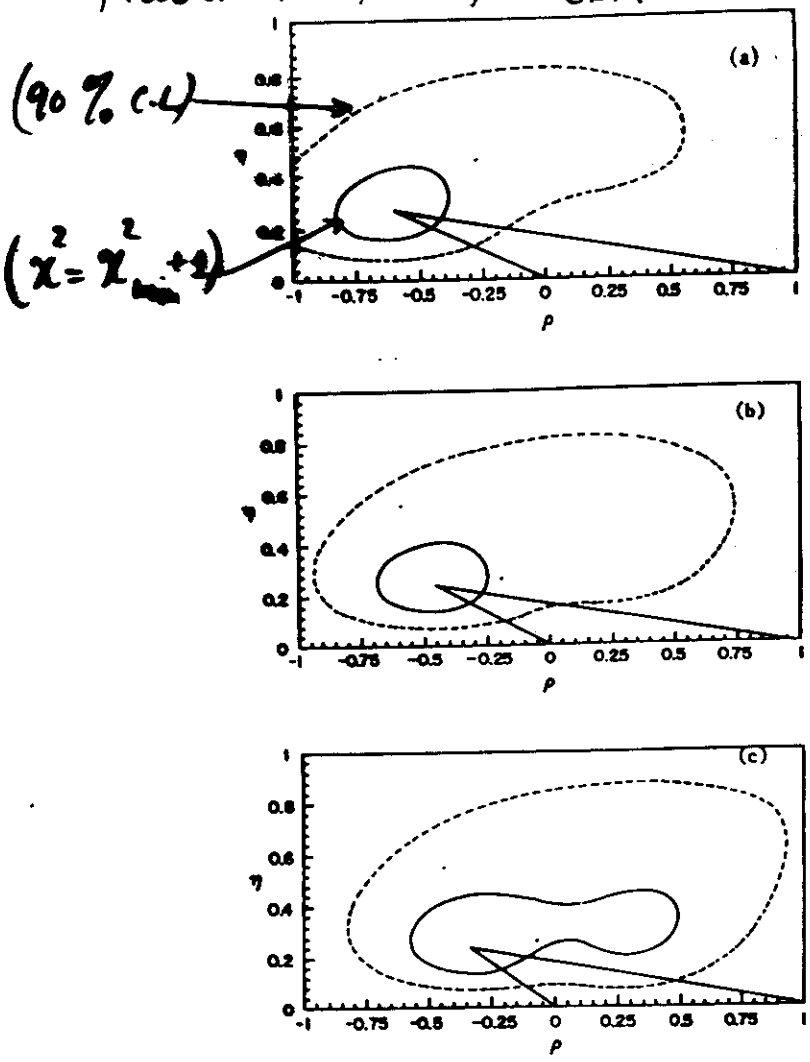

m_t = 100 GeV

140 GeV

180 GeV

Figure 4: Allowed region in ρ-η space for different values of the standard model parameters. Figs. (a)-(c) have $f_{B_d}\sqrt{B_{B_d}} = 135 \pm 25$ MeV, with $m_t = 100$, 140 and 180 GeV, respectively. The solid line represents the region with $\chi^2 = \chi^2_{min} + 1$; the dashed line denotes the 90% c.l. region. The triangles show the best fit.

$$f_{B_d}\sqrt{B_d} = (135 \pm 25^{14}) \text{ MeV}$$

Present Status of Δ_{CKM} (London, A.A.)

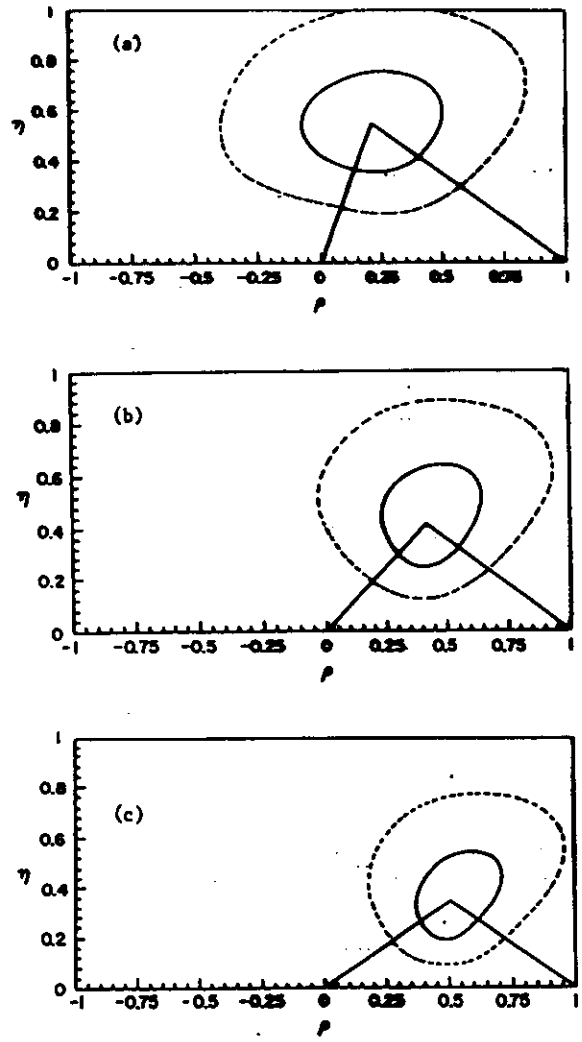

m_t = 100 GeV

140 GeV

180 GeV

Figure 5: Allowed region in ρ-η space for different values of the standard model parameters. Figs. (a)-(c) have $f_{B_d}\sqrt{B_{B_d}} = 240 \pm 40$ MeV, with $m_t = 100$, 140 and 180 GeV, respectively. The solid line represents the region with $\chi^2 = \chi^2_{min} + 1$; the dashed line denotes the 90% c.l. region. The triangles show the best fit.

$$f_{B_d}\sqrt{B_{B_d}} = (240 \pm 40)\ \text{MeV}$$

"Best fits" of (ρ, η) (London, A.A.)

m_t(GeV)	c_d (MeV)	(ρ, η)	χ^2_{min}
100	125 ± 20	$(-0.6, 0.27)$	0.05
140		$(-0.47, 0.25)$	0.55
180		$(-0.34, 0.25)$	2.1
100	225 ± 30	$(0.22, 0.54)$	0.20
140		$(0.42, 0.42)$	0.10
180		$(0.51, 0.34)$	0.02

$$c_d \equiv f_{B_d}\sqrt{B_{B_d}\eta_B}$$

Determination of Wolfenstein-CKM Parameters

$$A = 0.90 \pm 0.12$$

$$\lambda = 0.2205 \pm 0.0018$$

$$0.25 \leq \eta \leq 0.54$$

$$-0.60 \leq \rho \leq 0.51$$

(with $\sqrt{\rho^2+\eta^2}$ ✱ $= 0.63 \pm 0.23$)

Standard model prediction for x_s

The SM expression for x_s is

$$x_s = \tau_{B_s} \frac{G_F^2}{6\pi^2} M_W^2 M_{B_s} \left(f_{B_s}^2 B_{B_s}\right) \eta_{B_s} A^2 \lambda^4 y_t f_2(y_t)$$

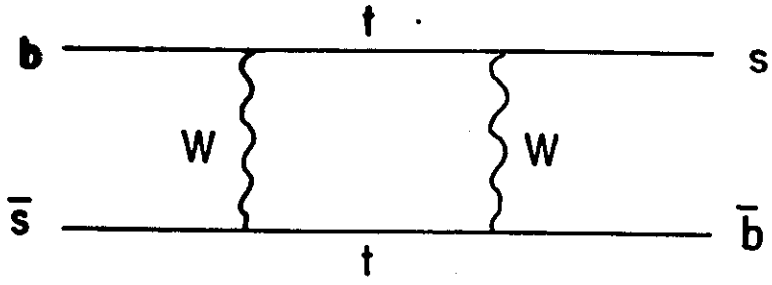

Figure 6: Box diagram for B_s^0-$\overline{B_s^0}$ mixing. There is another diagram in which the internal t-quark and W lines are interchanged.

Using the fact that $V_{cb} = V_{ts}$ it is clear that one of the sides of the unitarity triangle, $|V_{td}/\lambda V_{cb}|$, can be obtained from the ratio of x_d and x_s:

$$\frac{x_d}{x_s} = \frac{\tau_{B_d}\eta_{B_d} M_{B_d}\left(f_{B_d}^2 B_{B_d}\right)}{\tau_{B_s}\eta_{B_s} M_{B_s}\left(f_{B_s}^2 B_{B_s}\right)} \left|\frac{V_{td}}{V_{ts}}\right|^2$$

$$\simeq (1.1 - 1.4) \left|\frac{V_{td}}{V_{ts}}\right|^2$$

$x_s \Rightarrow$ det. of $|V_{td}/V_{ts}|$

SM Estimates: $x_s \simeq \mathcal{O}(15)$

time-dependent ~ 1

[H. Schröder]

$$\chi_i = \frac{x_i^2}{2(x_i^2+1)} \xrightarrow{x_i \gg 1} 1/2$$

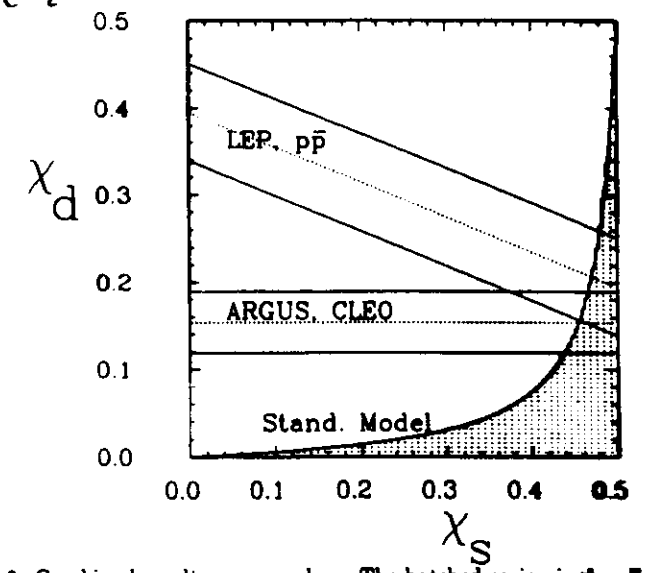

$\chi = 0.118 \pm 0.018$

$\chi_d = 0.155 \pm 0.030$

$\Rightarrow$

$x_d = 0.67 \pm 0.1$

Figure 6: Combined results on χ_d and χ_s. The hatched region is the allowed range for the limit $|V_{td}|^2 / |V_{ts}|^2 < 0.21$ which is derived from the unitarity of the KM matrix with three families.

we will use:

$$\chi = 0.375 \cdot \chi_d + 0.15 \cdot \chi_s \tag{51}$$

Comparing the results from the Z^0 and from the continuum with the ARGUS and CLEO result one finds excellent agreement if χ_s is large (Figure 6). With the chosen values for p_d and p_s the measurements imply a value of $\chi_s > 0.37$. The values of χ_d and χ_s are related by

$$\frac{x_d}{x_s} = \frac{\sqrt{\frac{2\chi_d}{1-2\chi_d}}}{\sqrt{\frac{2\chi_s}{1-2\chi_s}}} \approx \frac{|V_{td}|^2}{|V_{ts}|^2} \tag{52}$$

assuming equal B decay constants. From the measurement of χ_d and the limit for $|V_{td}|^2 / |V_{ts}|^2 < 0.21$ derived from the unitarity of the KM-matrix[25] , it is possible to obtain an ever stronger constraint on $\chi_s > 0.44$ (Figure 6). The measurement of χ from the high energy experiments does not improve this limit since the uncertainties in p_d and in particular p_s are too large. Similarly the χ measurement does not give additional information on χ_d but is very consistent with the measurement by ARGUS and CLEO.

Time-dependent B_s^0-$\overline{B_s^0}$ oscillations: formalism

Concentrating on the B_s^0-$\overline{B_s^0}$ system, the modulated time dependence of the single-meson state $|B_s^0 \to B_s^0; t|$ and the charged conjugate state produced due to mixing $|B_s^0 \to \overline{B_s^0}; t|$ are given by:

$$|B_s^0(t)\rangle = e^{-t/\tau_B} \cos^2(\frac{x_s t}{2\tau_B}) |B_s^0; t=0\rangle,$$

$$|\overline{B_s^0}(t)\rangle = e^{-t/\tau_B} \sin^2(\frac{x_s t}{2\tau_B}) |B_s^0; t=0\rangle.$$

For the $C = -1$ states the opposite-sign and like-sign states have the following differential (in time) probabilities:

$$P(B^0\overline{B^0};\, t_1, t_2) = \exp(-(t_1+t_2)/\tau_B) \cos^2(\frac{x(t_1-t_2)}{2\tau_B}),$$

$$P(B^0 B^0;\, t_1, t_2) = \exp(-(t_1+t_2)/\tau_B) \sin^2(\frac{x(t_1-t_2)}{2\tau_B}).$$

For the $C = +1$ states, the corresponding time evolution is given by:

$$P(B^0\overline{B^0}; t_1, t_2) = \exp(-(t_1+t_2)/\tau_B) \cos^2(\frac{x(t_1+t_2)}{2\tau_B}),$$

$$P(B^0 B^0; t_1, t_2) = \exp(-(t_1+t_2)/\tau_B) \sin^2(\frac{x(t_1+t_2)}{2\tau_B}).$$

Since the beam interaction point in the beam direction is not known accurately, t_1 and t_2 can not be determined individually. However, the proper time difference $|t_1 - t_2|$ can be measured. Integrating over the variable $t_1 + t_2$, one gets the following distribution in the time difference interval $\delta t = |t_1 - t_2|$ [89]:

$$P(B^0\overline{B^0}; \delta t) = \exp(-\delta t/\tau_B) \cos^2(\frac{x}{2}\frac{\delta t}{\tau_B}); \quad C = -1,$$

$$P(B^0 B^0 + \overline{B^0}\,\overline{B^0}; \delta t) = \exp(-\delta t/\tau_B) \sin^2(\frac{x}{2}\frac{\delta t}{\tau_B}); \quad C = -1,$$

$$P(B^0\overline{B^0}; \delta t) = \frac{1}{2}\frac{1}{1+x^2} \exp(-\delta t/\tau_B)\{2\cos^2(\frac{x}{2}\frac{\delta t}{\tau_B}) + x^2 - x\sin(x\frac{\delta t}{\tau_B})\}; \quad C = -$$

$$P(B^0 B^0 + \overline{B^0}\,\overline{B^0}; \delta t) = \frac{1}{2}\frac{1}{1+x^2} \exp(-\delta t/\tau_B)\{2\sin^2(\frac{x}{2}\frac{\delta t}{\tau_B}) + x^2 + x\sin(x\frac{\delta t}{\tau_B})\}; \quad C = -$$

x_s - measurement @ LEP

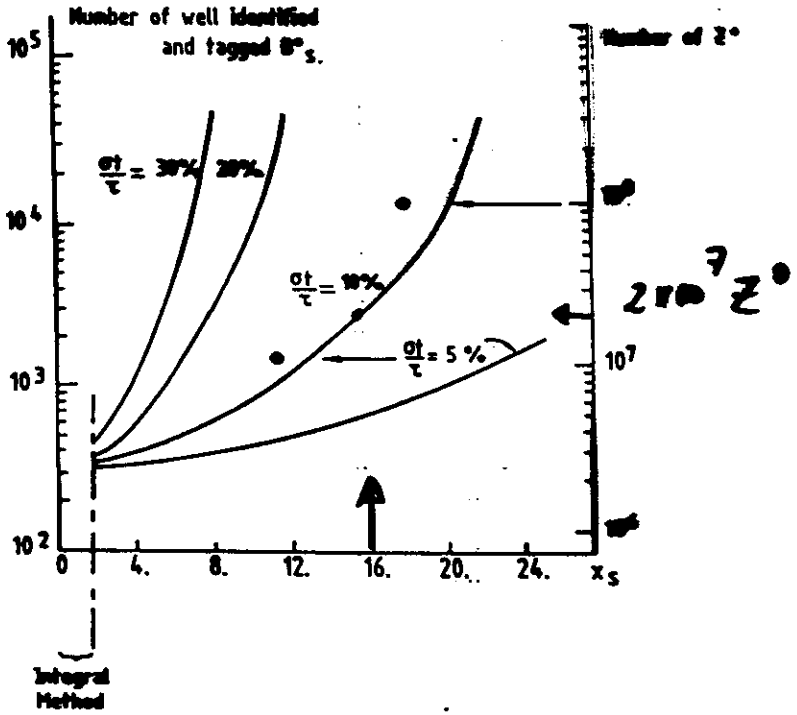

Figure 15: Estimates of the required number of Z^0's to measure x_s at LEP. The assumed value of the proper time resolution is indicated on the curves. Also shown are estimates of the corresponding number of well identified and tagged B^0_s for the DELPHI detector (from ref. [94]).

DESY 92-058
April 1992

Rare B-Decays in QCD

Ahmed Ali

Deutsches Elektronen Synchrotron - DESY
Hamburg, Germany

Abstract

We review theoretical work done on rare B-decays in the context of the Standard Model (SM) of electroweak interactions. The framework used is that of QCD, which is applied to calculate the decay rates and distributions in a number of processes, such as $B \to X_s + \gamma$, $B \to X_d + \gamma$, $B \to X_s + \ell^+\ell^-$, and $B \to X_s + \nu\bar{\nu}$, where X_s and X_d denote light hadrons with an overall quantum number $S = -1$ and $S = 0$, respectively. We particularly emphasise inclusive measurements in this sector, which would eventually permit a more reliable comparison of the SM predictions and experiments. However, we also discuss estimates of some exclusive rare B-decay modes, calculated in the vector meson dominance approximation and using the heavy quark effective theory (HQET). The importance of measuring the CKM-suppressed rare B-decays in determining the CKM matrix-element V_{td} is underlined. Rate estimates in some inclusive and exclusive suppressed rare decay modes are presented by imposing current experimental constraints on the CKM matrix.

*To be published in the Proceedings of the 1991 ICTP, Trieste, Summer School in High Energy Physics and Cosmology, World Scientific Publishers, Singapore (1992).

2 RADIATIVE RARE B-DECAYS

We start by discussing the dominant FCNC inclusive B-decays. Such processes (as far as the short-distance contribution is concerned) are forbidden at the tree level in the SM Lagrangian but are allowed at the one-loop order. They have received quite a bit of theoretical interest in the last decade [25]-[44], since they serve both as precision tests of the Standard Model and windows on possible new physics. Here, we shall concentrate on the SM physics only and refer to a recent review covering the non-SM aspects of B-decays [45]. We enumerate the processes of interest in B-decays, define the effective Hamiltonians that govern them, and review the one-loop renormalisation group (RG) improvement of the relevant Wilson coefficients of the operators in these Hamiltonians. This framework is then employed to calculate the inclusive rates and the energy-momentum profile of the decay products, using perturbative QCD and a B-meson wave function model.

In terms of the quark transitions, the main FCNC B-decays are the following:

1. $b \to (s,d) + \gamma$
2. $b \to (s,d) + \gamma + g$
3. $b \to (s,d) + g$
4. $b \to (s,d) + \ell^+\ell^- \ (\ell = e,\mu)$
5. $b \to (s,d) + \nu\bar{\nu}$

Of these, the most difficult to measure experimentally are the ones involving the hadronic final states $b \to (s,d) + g$, since they don't have a clean signature to be detected from the dominating CC decays $b \to u\bar{u}d$. So, we shall mostly neglect them and concentrate on the rest in the above list. The QCD improvements are usually done in the framework of an effective theory obtained by integrating out the heavy degrees of freedom, namely the top quark and the $W^\pm$ bosons. To be precise, these corrections are calculated in the leading logarithm approximation (LLA) since only in this approximation does the effective theory (with 5 quarks) match with the full theory (with 6 quarks and the $W^\pm$-bosons). As it will become clear from the discussion below, this matching is done in terms of the Wilson coefficients of the operators entering the effective Hamiltonian. This improved effective Hamiltonian incorporating the leading order RG-improvement is the basis of all phenomenological studies presented here. We remark that the gluon bremsstrahlung corrections, such as $b \to (s,d)+\gamma+g$, are required to get non-trivial photon energy spectra. Incorporating the QCD bremsstrahlung corrections and the virtual correction to $b \to (s,d) + \gamma$, using the one-loop improved effective Hamiltonian, amounts to incorporating the next-to leading order QCD corrections in the decays $B \to X_s + \gamma$ and $B \to X_d + \gamma$. The next-to-leading order corrections modify the rates for the inclusive decays $B \to X_d + \gamma$ and $B \to X_s + \gamma$, and their quantitative estimates are discussed below.

2.1 The Decays $b \to (s,d) + \gamma$: Lowest Order Contributions

We start with the lowest order (1-loop) calculations for the FCNC radiative decays $b \to (s,d) + \gamma$. Due to their similarity with the transitions $b \to s + X$ we shall discuss the

$b \to d + X$ transitions only when there are non-trivial differences. The matrix element for the process $b \to s + \gamma$ in the lowest order can be written as:

$$\mathcal{M}(b \to s\ +\gamma) = \frac{G_F}{\sqrt{2}}\frac{e}{2\pi^2}\sum_i V_{ib}V_{is}^* F_2^i(x_i)\, q^\mu \epsilon^\nu \bar{s}\sigma_{\mu\nu}(m_b R\ +\ m_s L)b \qquad (1)$$

where G_F is the Fermi coupling constant, $L = (1-\gamma_5)/2$, $R = (1+\gamma_5)/2$, $x_i = m_i^2/m_W^2$, q_μ and ϵ_μ are, respectively, the photon four-momentum and polarisation vector, and the sum is over the quarks, u, c, and t. The CKM matrix elements V_{ij} appearing above are defined in the Wolfenstein parametrisation [46]:

$$V_{\rm CKM-W} = \begin{pmatrix} 1-\frac{1}{2}\lambda^2 & \lambda & A\lambda^3(\rho - i\eta) \\ -\lambda & 1-\frac{1}{2}\lambda^2 & A\lambda^2 \\ A\lambda^3(1-\rho-i\eta) & -A\lambda^2 & 1 \end{pmatrix} \qquad (2)$$

The representation, $V_{\rm CKM-W}$, has three real parameters A, λ, and ρ, and a phase η, whose current values will be discussed below. The Inami-Lim function $F_2(x_i)$ derived from the penguin diagrams is given by [47]:

$$F_2(x) = \frac{x}{24(x-1)^4}\left[6x(3x-2)\log x - (x-1)(8x^2+5x-7)\right] \qquad (3)$$

where we have dropped the superscript on F_2, and in writing the expression for $F_2(x_i)$ above we have left out terms of order $O(m_s/m_b)$. For small x_i one has $F_2(x_i) \sim x_i$, hence the contribution of the u and c quarks in Eq. (1) can be neglected. Retaining only the top quark contribution in the amplitude, we have:

$$\mathcal{M}(b \to s\ +\gamma) = \frac{G_F}{\sqrt{2}}\frac{e}{2\pi^2}\lambda_t F_2(x_t)\, q^\mu \epsilon^\nu \bar{s}\sigma_{\mu\nu}(m_b R\ +\ m_s L)b \qquad (4)$$

with $\lambda_t \equiv V_{tb}V_{ts}^*$. The amplitude for the CKM-suppressed FCNC radiative transition $b \to d + \gamma$ is obtained by replacing the s-quark variables by the d-quark ones. The CKM factor in this case is $\xi_t \equiv V_{tb}V_{td}^*$. The widths $\Gamma(b \to s + \gamma)$ and $\Gamma(b \to d + \gamma)$ in the lowest order are:

$$\Gamma(b \to s + \gamma) = |\lambda_t|^2 \frac{G_F^2 m_b^5 \alpha}{32\pi^4}|F_2(x_t)|^2 \qquad (5)$$

$$\Gamma(b \to d + \gamma) = |\xi_t|^2 \frac{G_F^2 m_b^5 \alpha}{32\pi^4}|F_2(x_t)|^2 \qquad (6)$$

where we have dropped terms of $O(m_s/m_b)$ and $O(m_d/m_b)$ in the phase space also. From the expression for $F_2(x_t)$ it is easy to see that for low values of x_t ($x_t \ll 1$) one has a quartic suppression in m_t of the decay rates $\Gamma(b \to s + \gamma)$ and $\Gamma(b \to d + \gamma)$; this goes over to a constant behaviour for $x_t \gg 1$. So, while intrinsically there is a large m_t-dependence in the decay widths for both the $b \to s + \gamma$ and $b \to d + \gamma$ transitions, this dependence in the m_t-range of present phenomenological interest, 100 GeV $< m_t <$ 200 GeV, is rather modest, as can be seen in Fig. 1.

The rates for rare B-decays may be expressed in terms of the branching ratio for the inclusive CC semileptonic B-decays $B \to (X_c,\ X_u)\ell\nu_\ell$, which have been well measured

Grenb, A.J.

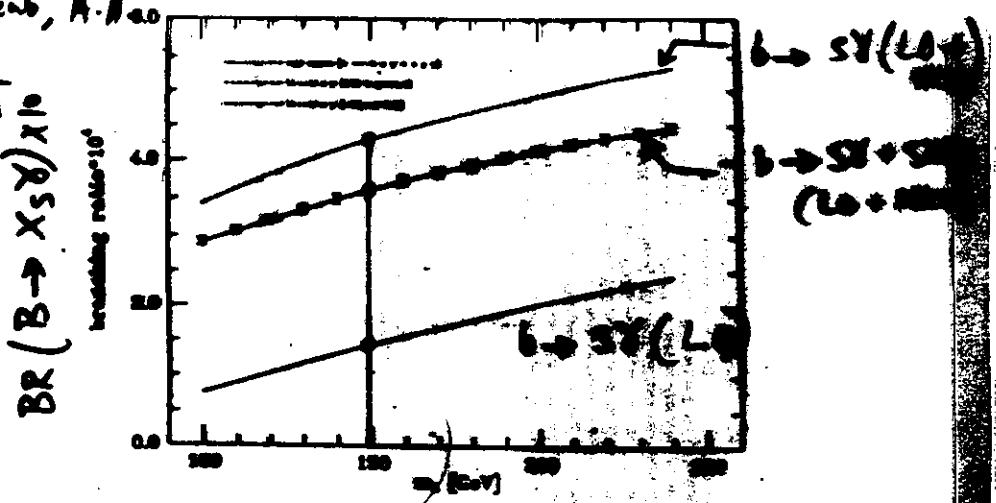

Figure 1: Inclusive branching ratio for the decays $B \to X_s\gamma$ as a function of the top-quark mass m_t. The charm quark mass dependence for $m_c =$ [illegible] bars. Also shown are the lowest order (i.e. without QCD [illegible] the leading-order QCD-improved results for the two-body decays $b \to s + \gamma$ [illegible]

(here and henceforth we use the quark flavour in the transition $b \to q\gamma$ to specify the resulting hadronic state, X_q). This removes the annoying m_b^5 dependence in their ratios. In the approximation of keeping the dominant $b \to c\bar{u}_i$ contribution, one has:

$$BR(b \to s + \gamma) = 6\frac{\alpha}{\pi}\frac{|\lambda_t|^2}{|V_{cb}|^2}\frac{|R(s_0)|^2}{f(m_c/m_b)}(0.12) \qquad (7)$$

$$\frac{BR(b \to d + \gamma)}{BR(b \to s + \gamma)} = \frac{|V_{td}|^2}{|V_{ts}|^2} \qquad (8)$$

where the function $f(m_c/m_b)$ is the the phase space factor in the CC semileptonic decay $b \to c + \bar{u}_i$. Numerically, $f(m_c/m_b) \simeq 0.44$. The number in the parenthesis in Eq. (7) corresponds to the average B-hadron semileptonic branching ratio given in the PDG tables [13]. The branching ratio for $b \to s + \gamma$ as a function of m_t is shown in Fig. 1, and we note that it does not depend on the CKM-matrix elements since $|V_{ts}|^2/|V_{cb}|^2 = 1$. To quote a number from this figure, one gets $BR(b \to s + \gamma) \simeq 3.5 \times 10^{-4}$ for $m_t = 180$ GeV, for the lowest order (i.e. no QCD corrections). We shall estimate the ratio in Eq. (8) later, making use of the available constraints on the CKM matrix elements. As an order of magnitude, we expect this ratio to be $O(\lambda^3) \simeq 0.05$. We discuss first the leading order perturbative QCD corrections in the two-body decays $b \to (s,d) + \gamma$ [illegible] QCD renormalization of the Wilson coefficients) and then take up the next-to-leading order corrections due to the gluon bremsstrahlung contributions from the decays $b \to (s,d) + \gamma + g$, as well as, the virtual corrections to $b \to (s,d) + \gamma$. This will lead us to the discussion of the inclusive photon energy spectra.

QCD Corrections to $b \to s\gamma$

2-Loop Diagrams $O(\alpha_s)$

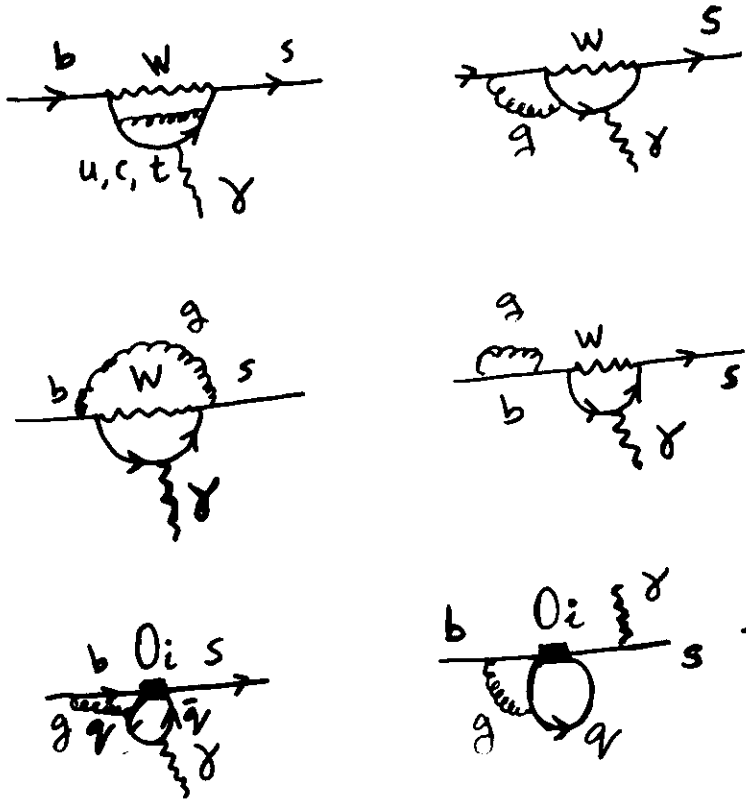

$$C_i(m_W) \longrightarrow C_i(\mu)$$
$$(\mu < m_W)$$

ld use the equations of motion to get rid of the covariant derivatives and reduce the number ıdependent operators. To leading order in the small (weak)-mixing angles, a complete set imension-6 operators relevant for the processes $b \to s+\gamma$ and $b \to s+\gamma+g$ is contained he effective Hamiltonian

$$H_{eff}(b \to s+\gamma) = -\frac{4G_F}{\sqrt{2}} \lambda_t \sum_{j=1}^{8} C_j(\mu)\, \hat{O}_j(\mu) \qquad (9)$$

h $C_j(\mu)$ being the Wilson coefficients evaluated at the scale μ. The various operators are ned as:

$$\begin{aligned}
\hat{O}_1 &= (\bar{c}_{L\beta}\gamma^\mu b_{L\alpha})(\bar{s}_{L\alpha}\gamma_\mu c_{L\beta}) \\
\hat{O}_2 &= (\bar{c}_{L\alpha}\gamma^\mu b_{L\alpha})(\bar{s}_{L\beta}\gamma_\mu c_{L\beta}) \\
\hat{O}_3 &= (\bar{s}_{L\alpha}\gamma^\mu b_{L\alpha}) \left[(\bar{u}_{L\beta}\gamma_\mu u_{L\beta}) + \cdots + (\bar{b}_{R\beta}\gamma_\mu b_{R\beta})\right] \\
\hat{O}_4 &= (\bar{s}_{L\alpha}\gamma^\mu b_{L\beta}) \left[(\bar{u}_{L\beta}\gamma_\mu u_{L\alpha}) + \cdots + (\bar{b}_{R\beta}\gamma_\mu b_{R\alpha})\right] \\
\hat{O}_5 &= (\bar{s}_{L\alpha}\gamma^\mu b_{L\alpha}) \left[(\bar{u}_{R\beta}\gamma_\mu u_{R\beta}) + \cdots + (\bar{b}_{R\beta}\gamma_\mu b_{R\beta})\right] \\
\hat{O}_6 &= (\bar{s}_{L\alpha}\gamma^\mu b_{L\beta}) \left[(\bar{u}_{R\beta}\gamma_\mu u_{R\alpha}) + \cdots + (\bar{b}_{R\beta}\gamma_\mu b_{R\alpha})\right] \\
\hat{O}_7 &= (e/16\pi^2)\, \bar{s}_\alpha\, \sigma^{\mu\nu}\, (m_b R + m_s L)\, b_\alpha\, F_{\mu\nu} \\
\hat{O}_8 &= (g_S/16\pi^2)\, \bar{s}_\alpha\, \sigma^{\mu\nu}\, (m_b R + m_s L)\, T^A_{\alpha\beta}\, b_\beta\, G^A_{\mu\nu}
\end{aligned} \qquad (10)$$

lag. lowest 0:

nd g_S denote the QED and QCD coupling constant, respectively. Perturbative QCD correc- ns, contained in the Wilson coefficients $C_j(\mu)$, have been evaluated to leading logarithmic uracy. It is known that the Wilson coefficients of the operators $\hat{O}_3, \ldots, \hat{O}_6$ get contributions m operator mixing only; as these coefficients are numerically small [20,26,27] their effect ısually neglected. The coefficients $C_1(\mu), C_2(\mu), C_7(\mu)$ and $C_8(\mu)$, obtained by integrating : the top quark and the W-boson simultaneously, are given in refs. [20,26]. At $\mu = m_b$, ich is the relevant scale for the b quark decay, these coefficients read as follows:

QCD Corrections

$$\begin{aligned}
C_1(m_b) &= \frac{1}{2}\left[\eta^{-6/23} - \eta^{12/23}\right] C_2(m_W) \\
C_2(m_b) &= \frac{1}{2}\left[\eta^{-6/23} + \eta^{12/23}\right] C_2(m_W) \\
C_7(m_b) &= \eta^{-16/23}\left\{C_7(m_W) - \frac{58}{135}\left[\eta^{16/23} - 1\right] C_2(m_W) - \frac{29}{189}\left[\eta^{39/23} - 1\right] C_8(m_W)\right\} \\
C_8(m_b) &= \eta^{-14/23}\left\{C_8(m_W) - \frac{11}{144}\left[\eta^{8/23} - 1\right] C_2(m_W) + \frac{35}{234}\left[\eta^{39/23} - 1\right] C_8(m_W)\right\}
\end{aligned} \qquad (11)$$

$$\eta = \frac{\alpha_S(\mu)}{\alpha_S(m_W)}, \qquad \mu \sim O(m_b)$$

(Bertolini et al., Grigjanis et al., Grinstein et al.,

Technique

use RGE to evaluate Wilson Coefficients $C_j(\mu)$ with $C_j(m_W)$ as boundary value functions

RGE

$$\mu \frac{d}{d\mu} C_j(\mu) - \sum_{i=1}^{8} \gamma_{ij}(g_s) C_i(\mu) = 0$$

Solution

$$C_j(\mu) = \left[\exp \int_{g_s(m_W)}^{g_s(\mu)} dg_s \, \frac{\gamma^T(g_s)}{\beta(g_s)}\right]_{ji} C_i(m_W)$$

Matching functions

$$C_i(m_W) = 0, \quad i = 1, 3, 4, 5, 6$$

$$C_2(m_W) = 1$$

$$C_7(m_W) = F_2(x); \quad x = m_t^2/m_W^2$$

$$C_8(m_W) = \frac{-x}{\ldots 4}\left[6x \ln x + (x-1)(x^2 - 5x - 2)\right.$$

Anomalous dimension Matrix $\hat{\gamma}$

(Grinstein et al.)

$$\gamma_{ij} = \frac{g_s^2}{8\pi^2}\,\hat{\gamma}_{ij}$$

N.B. Only operators O_1, O_2, O_7, O_8 are important + kept

$$\hat{\gamma}_{11} = -1$$
$$\hat{\gamma}_{12} = 3$$
$$\hat{\gamma}_{17} = 0$$
$$\hat{\gamma}_{18} = Y_1$$
$$\hat{\gamma}_{21} = 3$$
$$\hat{\gamma}_{22} = -1$$
$$\Rightarrow \quad \hat{\gamma}_{27} = X_2 = \frac{232}{81}$$
$$\hat{\gamma}_{28} = Y_2 \quad \text{(not needed for } b\to s\gamma\text{)}$$
$$\hat{\gamma}_{77} = \frac{16}{3}$$
$$\hat{\gamma}_{78} = 0$$
$$\hat{\gamma}_{87} = -16/9$$
$$\hat{\gamma}_{88} = 14/3$$

Mixing between $(O_1, \ldots, O_6)$ + (O_7, O_8)

RG-Improved $BR(b\to s\gamma)$ + $BR(b\to d\gamma)$

$$BR(b\to s\gamma) = \frac{6\alpha}{\pi f(m_c/m_b)} \left|C_7(m_b)\right|^2 \quad (0.12)$$

RG-Improvement: $C_7(m_W) \to C_7(m_b)$

$$C_7(\mu) = \eta^{16/23}\left\{C_7(m_W) - \frac{8}{3}C_8(m_W)\left(1-\eta^{2/23}\right) + \frac{3X_2}{19}\left(1-\eta^{19/23}\right)\right\}$$

$$\eta = \alpha_s(m_W)/\alpha_s(\mu) \;;\quad X_2 = \frac{232}{81}$$

$$\Rightarrow \boxed{BR(b\to s\gamma) = (3-4)\times 10^{-4}}$$

Babolini et al.; Grinstein et al.; Cella et al.; Misiak; ....

$$\frac{BR(b\to d\gamma)}{BR(b\to s\gamma)} = \frac{|V_{td}|^2}{|V_{ts}|^2}$$

Remains unrenormalized by RG-Corrections

$$\Downarrow$$

$$\frac{BR(B\to\rho\gamma)}{BR(B\to K^*\gamma)} = K\left|\frac{V_{td}}{V_{ts}}\right|^2$$

Rates + $BR(B \to X_d\gamma)$ + $BR(B \to \rho\gamma)$

- Including bremsstrahlung contributions

$$\frac{BR(B\to X_d\gamma)}{BR(B\to X_s\gamma)} = \frac{|\lambda_{td}|^2}{|\lambda_{ts}|^2}\left[K(m_t,\rho,\eta)\right]$$

$$K(m_t,\rho,\eta) = \left[1 - \frac{1-\rho}{|V_{td}|^2} D_2(x_t) - \frac{\eta}{|V_{td}|^2} D_3(x_t) + \frac{D_4(x_t)}{|V_{td}|^2}\right]$$

$\Rightarrow$ $BR(X_d\gamma)$ + $\frac{d\Gamma}{dx_\gamma}(B\to X_d\gamma)$ sensitive to (ρ,η)

*** $BR(B\to X_d\gamma) = (0.6-3)\times 10^{-5}$

*** $$\frac{BR(B\to\rho\gamma)}{BR(B\to K^*\gamma)} = 0.04\left[\frac{|V_{td}|^2}{5\times10^{-5}}\right]$$

independent of m_t!

- $BR(B\to\rho\gamma) = (1-3)\times 10^{-6}\left[\frac{(|V_{td}|)^2}{5\times10^{-5}}\right]$

(Model dependent)

$\mathcal{H}_{eff}(b\to d\gamma)$

Greub, A. A. DESY Report 92-048

$$\mathcal{H}_{eff}(b\to d\gamma) = -\frac{4G_F}{\sqrt{2}}\xi_t\sum_{j=1}^{8} C_j(\mu)\hat{O}_j(\mu)$$

$(\xi_i \equiv V_{ib}V_{id}^*)$

- $C_j(\mu)$ + $C_j(m_W)$ for $\mathcal{H}(b\to d\gamma)$ Same as in $\mathcal{H}_{eff}(b\to s\gamma)$ iff

$$\hat{O}_1 = -\frac{\xi_c}{\xi_t}(\bar{c}_\beta\gamma^\mu b_\alpha)_L(\bar{d}_\alpha\gamma_\mu c_\beta)_L - \frac{\xi_u}{\xi_t}(\bar{u}_\beta\gamma^\mu b_\alpha)_L(\bar{d}_\alpha\gamma_\mu u_\beta)_L$$

$$\hat{O}_2 = -\frac{\xi_c}{\xi_t}(\bar{c}_\alpha\gamma^\mu b_\alpha)_L(\bar{d}_\beta\gamma_\mu c_\beta) - \frac{\xi_u}{\xi_t}(\bar{u}_\alpha\gamma^\mu b_\alpha)_L(\bar{d}_\beta\gamma_\mu u_\beta)_L$$

$\hat{O}_i(b\to d\gamma) = O_i(b\to s\gamma)$ $\quad i=3,\dots,8$

(with $d\leftrightarrow s$)

$m_t(GeV)$	D_1	D_2	D_3	D_4
100	0.15	0.21	0.05	0.14
120	0.17	0.20	0.06	0.13
140	0.18	0.18	0.06	0.12
160	0.19	0.17	0.04	0.11
180	0.20	0.17	0.03	0.10
200	0.21	0.16	0.03	0.10

Table 1: Values of the coefficients D_i entering in Eq. (28) as a function of m_t.

$$BR(B \to \rho\gamma) \simeq (2-5)\times 10^{-6}\left(\frac{|V_{td}|}{9\times 10^{-3}}\right)^2$$

$m_t(GeV) =$	100	140	200
$p_T = 0.21\ GeV$	3.2	3.8	4.6
$p_T = 0.30\ GeV$	2.4	2.9	3.4
$p_T = 0.39\ GeV$	2.0	2.4	2.8

Table 2: Branching Ratio for the decay $B \to \rho + \gamma$ in units of $10^{-6} \times (|V_{td}|^2/7.78 \cdot 10^{-6})$

$$BR(B \to K^*\gamma) \simeq (3-8)\times 10^{-5}$$

$m_t(GeV) =$	100	140	200
$p_T = 0.21\ GeV$	5.4	6.5	7.8
$p_T = 0.30\ GeV$	3.9	4.8	5.7
$p_T = 0.39\ GeV$	3.1	3.8	4.5

Table 3: Branching Ratio for the decay $B \to K^* + \gamma$ in units of 10^{-5}

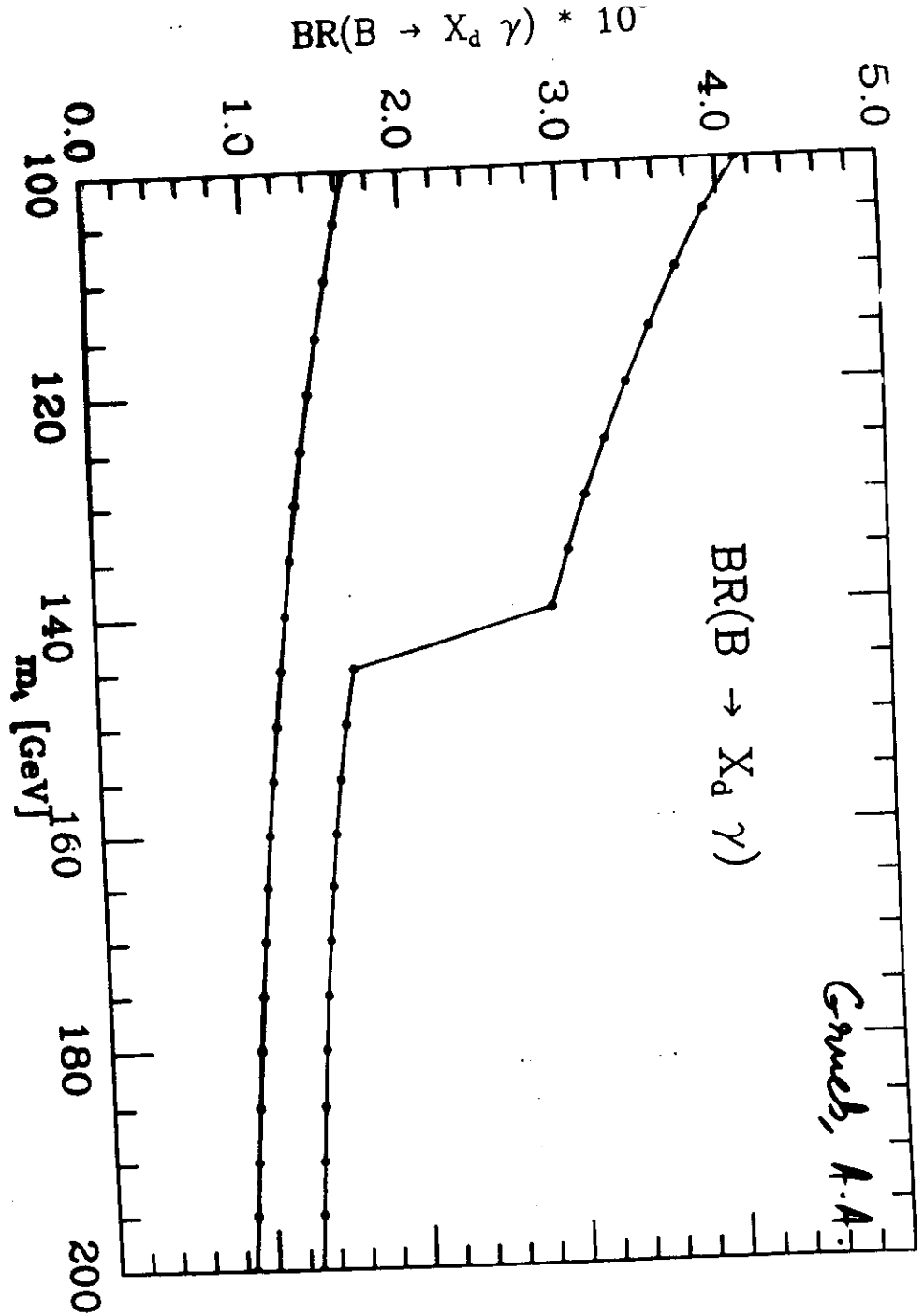

DESY 92-089
ZU-TH 23/92
June 1992

Prompt Photon Energy Spectra in B-Decays and Determination of the CKM Matrix Elements

A. Ali

Deutsches Elektronen Synchrotron DESY, Hamburg, Germany

C. Greub [1]

Universität Zürich, Zürich, Switzerland

Abstract

We present theoretical estimates of the inclusive prompt photon energy spectrum in direct decays of B-hadrons through the charged current processes $B \to X_c + \gamma$ and $B \to X_u + \gamma$, and the flavour changing neutral current (FCNC) processes $B \to X_s + \gamma$ and $B \to X_d + \gamma$. Here the subscript q on X_q denotes the quark flavour in the transition $b \to q\gamma$. It is argued that the various components in the inclusive spectrum can, in principle, be disentangled using the photon energy and flavour tagging the hadron(s) recoiling against the photon in B-decays, thereby providing a new technique to determine the CKM matrix elements $|V_{cb}|, |V_{ub}|, |V_{ts}|$ and $|V_{td}|$. In particular, the high energy part of the inclusive photon energy spectrum is dominated by the electromagnetic penguins could provide the first direct measurement of the CKM matrix element $|V_{ts}|$. We quantify this by firming up predictions for the inclusive decays $B \to X_s + \gamma$ in the Standard Model.

[1] partially supported by Schweizerischer Nationalfonds.

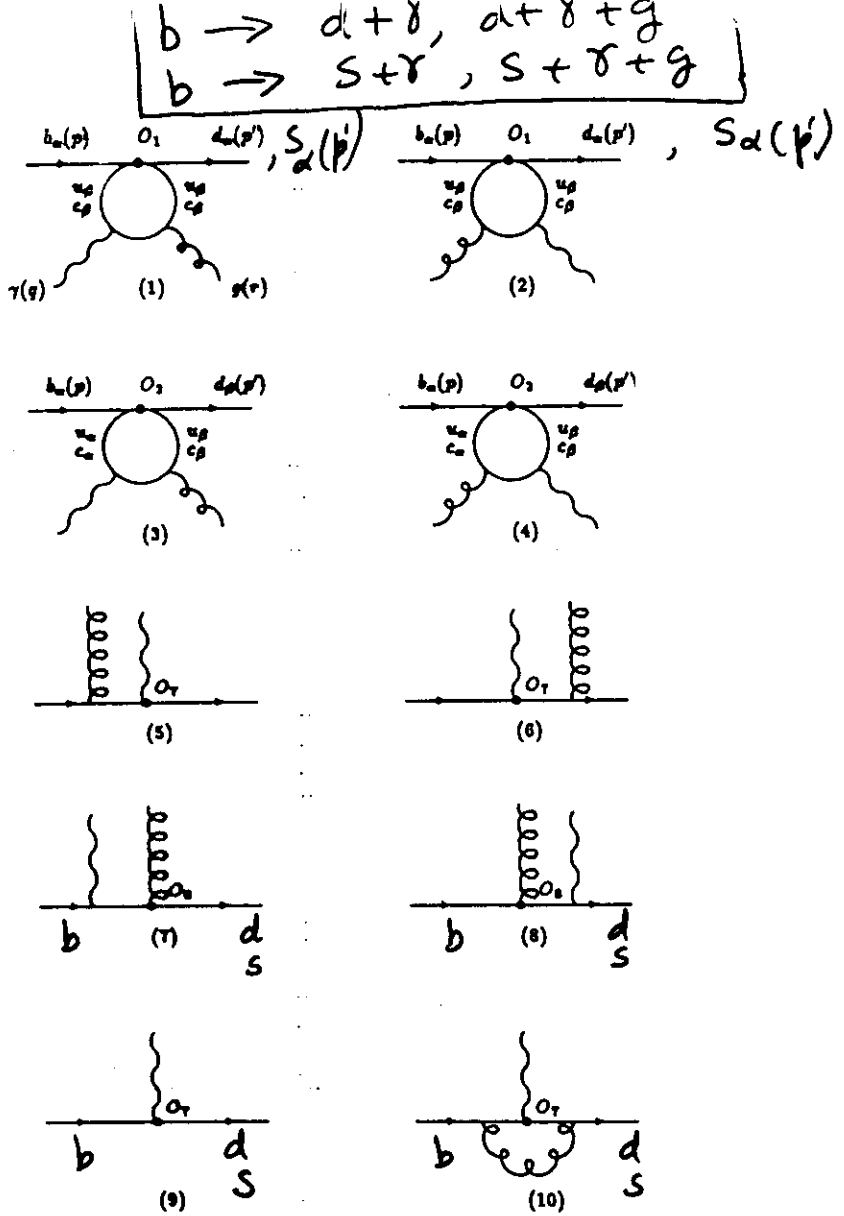

Figure 1

We define the kinematics of the CC radiative B-decays on the example of reaction $n = 1$ in Table 1,

$$b(p_1) \to c(p_2) + d(p_3) + \bar{u}(p_4) + \gamma(k). \tag{2}$$

The fully differential decay width for a b quark decaying at rest reads:

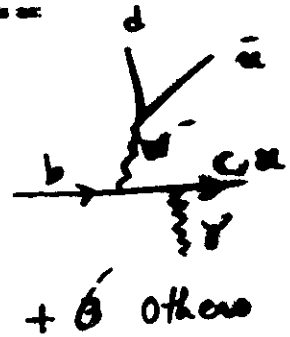

n	reaction	K_n
1	$b \to c\, d\bar{u}\gamma$	$3\,\lvert V_{cd}\rvert^2 \lvert V_{ud}\rvert^2$
2	$b \to c\, d\bar{c}\gamma$	$3\,\lvert V_{cd}\rvert^2 \lvert V_{cd}\rvert^2$
3	$b \to c\, s\bar{u}\gamma$	$3\,\lvert V_{cs}\rvert^2 \lvert V_{us}\rvert^2$
4	$b \to c\, s\bar{c}\gamma$	$3\,\lvert V_{cs}\rvert^2 \lvert V_{cs}\rvert^2$
5	$b \to c\, e^-\bar{\nu}_e\gamma$	$\lvert V_{cb}\rvert^2$
6	$b \to c\, \mu^-\bar{\nu}_\mu\gamma$	$\lvert V_{cb}\rvert^2$
7	$b \to c\, \tau^-\bar{\nu}_\tau\gamma$	$\lvert V_{cb}\rvert^2$
8	$b \to u\, d\bar{u}\gamma$	$3\,\lvert V_{ub}\rvert^2 \lvert V_{ud}\rvert^2$
9	$b \to u\, d\bar{c}\gamma$	$3\,\lvert V_{ub}\rvert^2 \lvert V_{cd}\rvert^2$
10	$b \to u\, s\bar{u}\gamma$	$3\,\lvert V_{ub}\rvert^2 \lvert V_{us}\rvert^2$
11	$b \to u\, s\bar{c}\gamma$	$3\,\lvert V_{ub}\rvert^2 \lvert V_{cs}\rvert^2$
12	$b \to u\, e^-\bar{\nu}_e\gamma$	$\lvert V_{ub}\rvert^2$
13	$b \to u\, \mu^-\bar{\nu}_\mu\gamma$	$\lvert V_{ub}\rvert^2$
14	$b \to u\, \tau^-\bar{\nu}_\tau\gamma$	$\lvert V_{ub}\rvert^2$

Table 1: CC radiative b-quark decays contributing to $B \to (X_c, X_u) + \gamma$ and their CKM matrix element dependent factors K_n.

$$d\Gamma_n = \frac{(2\pi)^4}{2m_b}\,\delta^4(p_1 - p_2 - p_3 - p_4 - k)\,\overline{|M_n|^2}\,d\mu(p_2)\,d\mu(p_3)\,d\mu(p_4)\,d\mu(k), \tag{3}$$

where the sum over the final spin and colour factors and average over the initial spin and colour are implied. The symbol $d\mu(p)$ defines the invariant measure for each particle in the final state, $d\mu(p) = d^3p/((2\pi)^3\,2p^0)$. The spin- and colour-averaged matrix element squared can be expressed as:

$$\boxed{\overline{|M_n|^2} = 128\,\pi\,\alpha_{em}\,G_F^2\,|A|^2\,K_n.} \tag{4}$$

Here K_n is a reaction dependent factor given in Table 1 and the reduced matrix element squared $|A|^2$ is given below:

$$\begin{aligned}
|A|^2 &= 2p_2\cdot p_3\left(\frac{Q_1^2}{p_1\cdot k}p_4\cdot k + \frac{Q_4^2}{p_4\cdot k}p_1\cdot k\right) + 2p_3\cdot p_4\left(\frac{Q_2^2}{p_2\cdot k}p_2\cdot k + \frac{Q_3^2}{p_3\cdot k}p_3\cdot k\right)\\
&\quad -4\,(Q_2Q_3p_1\cdot p_4 - Q_1Q_4p_2\cdot p_3) - p_3\cdot p_4\left(\frac{Q_1}{p_1\cdot k} + \frac{Q_4}{p_4\cdot k}\right)(B\cdot p_2p_3\cdot k - B\cdot p_2p_3\cdot k)\\
&\quad -p_1\cdot p_4\left(\frac{Q_2}{p_2\cdot k} - \frac{Q_3}{p_3\cdot k}\right)(B\cdot p_2p_3\cdot k - B\cdot p_2p_3\cdot k) - \frac{1}{2}B\cdot B p_2\cdot p_3p_4\cdot p_3 \ .
\end{aligned} \tag{5}$$

[15,16]. The branching ratio for the both the CC and FCNC radiative decays are calculated using the total B-decay width, Γ_{tot}:

$$\begin{aligned}
\Gamma_{tot} &= \left(r_u\,|V_{ub}|^2 + r_c\,|V_{cb}|^2\right)\Gamma_0\\
\Gamma_0 &= \frac{W_{eff}^5\,G_F^2}{192\pi^3} \quad ; \quad r_u \approx 7 \quad ; \quad r_c \approx 3
\end{aligned} \tag{11}$$

The values of r_u and r_c include phase space and QCD corrections [7,17]. The dependence on the effective b-quark mass, W_{eff}, which enters as the 5th power in both Γ_{tot} and all the radiative decays considered here cancels to a very large extent in the respective branching ratios. Note that the spectra and all the decay rates are calculated directly in term of the B-meson mass. The effective b-quark mass, entering in Γ_{tot}, can also be expressed in terms of the B-meson mass and the parameter p_F. A very good (numerical) functional dependence of W_{eff} for the present model can be parametrised as:

$$W_{eff}^2 \simeq M_B^2 - 2M_B\cdot p_F\cdot 1.28 \tag{12}$$

In the numerical estimates, a number of quark and lepton masses and the CKM matrix elements are needed. For the CKM matrix, we always use the Wolfenstein parametrization [18]. The explicit form of this matrix and an update of the actual values of the CKM matrix elements can be seen in [19]. Unless stated otherwise, the parameters used in our analysis are listed in Table 2, and the others are taken from the PDG tables [20].

The inclusive photon energy spectra from the CC radiative decays including the B-meson wave function effects are plotted in Figs. 1 a)– 1 c), corresponding to the non-leptonic decays, semileptonic decays and their sum, respectively. In each of these figures, we show the contribution from the decays $B \to X_c + \gamma$, $B \to X_u + \gamma$ and their sum $B \to (X_c, X_u) + \gamma$, as well as, the contributions from the FCNC processes $B \to X_s + \gamma$ and $B \to X_d + \gamma$ (discussed in the next section). We postpone a discussion of these spectra to section 4.

Parameter	Default value
$m_t\ (GeV)$	140
$m_c\ (GeV)$	1.68
$m_s\ (GeV)$	0.50
$m_u = m_d\ (GeV)$	0.30
$\mu\ (GeV)$	5.0
$\Lambda^{(5)}\ (GeV)$	0.225
$p_F\ (GeV)$	0.3
$\lvert V_{ts}\rvert$	0.041
$\lvert V_{cb}\rvert$	0.041
$\lvert V_{ub}\rvert/\lvert V_{cb}\rvert$	0.14
$\lvert V_{cd}\rvert = \lvert V_{us}\rvert$	0.220
$\lvert V_{cs}\rvert = \lvert V_{ud}\rvert$	0.975

Table 2: List of parameters and their default values used in the numerical estimates of the B-decay rates and photon energy spectra.

Grenb, A.A.

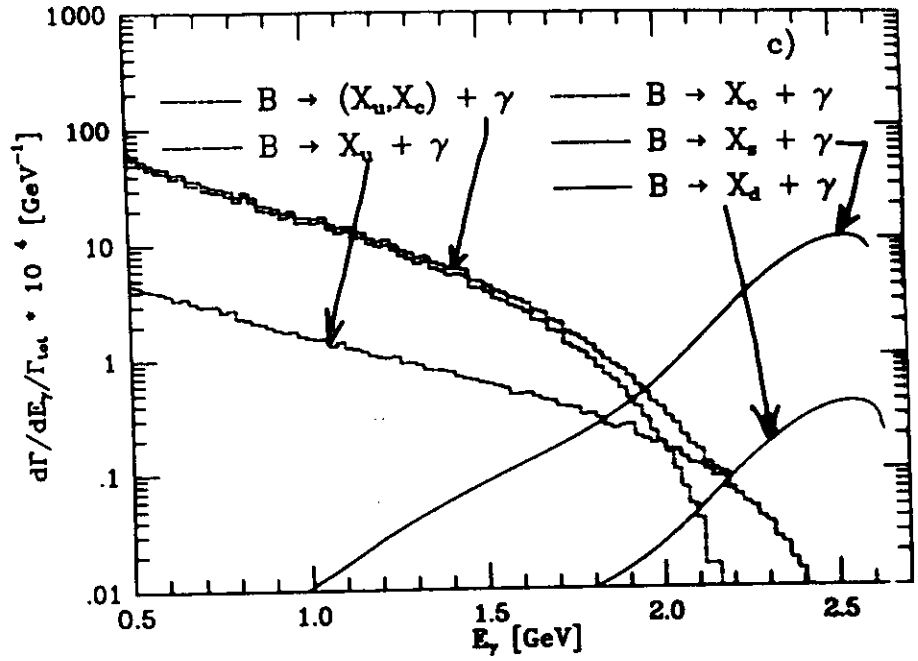

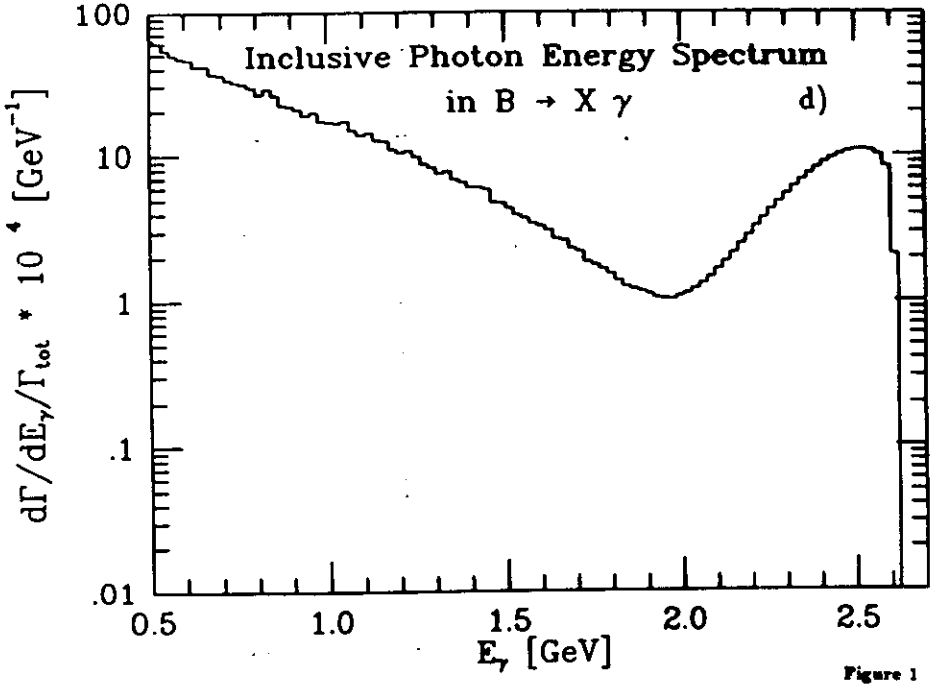

Figure 1

Grenb, A.A.

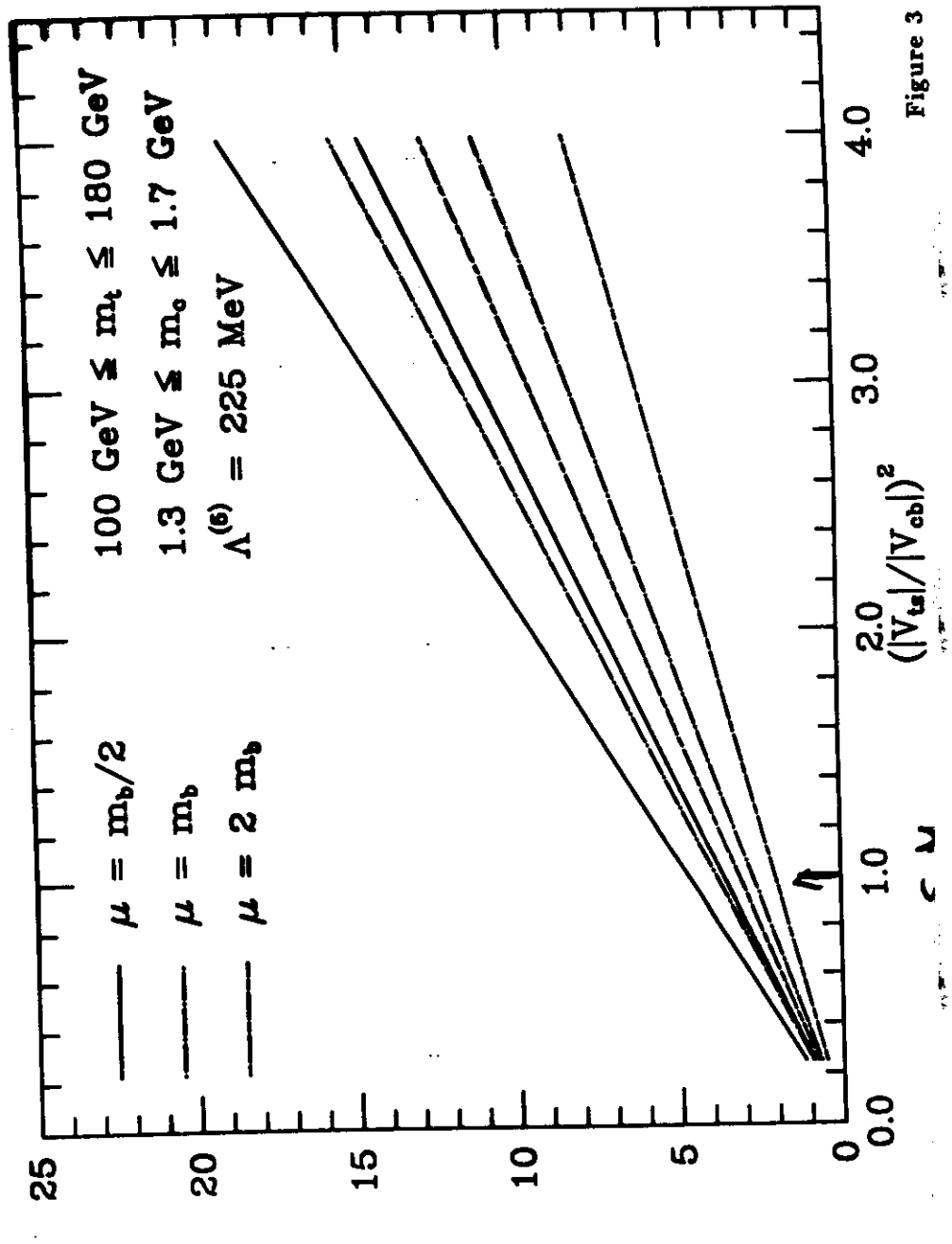

Figure 3

Grunb, A.A.

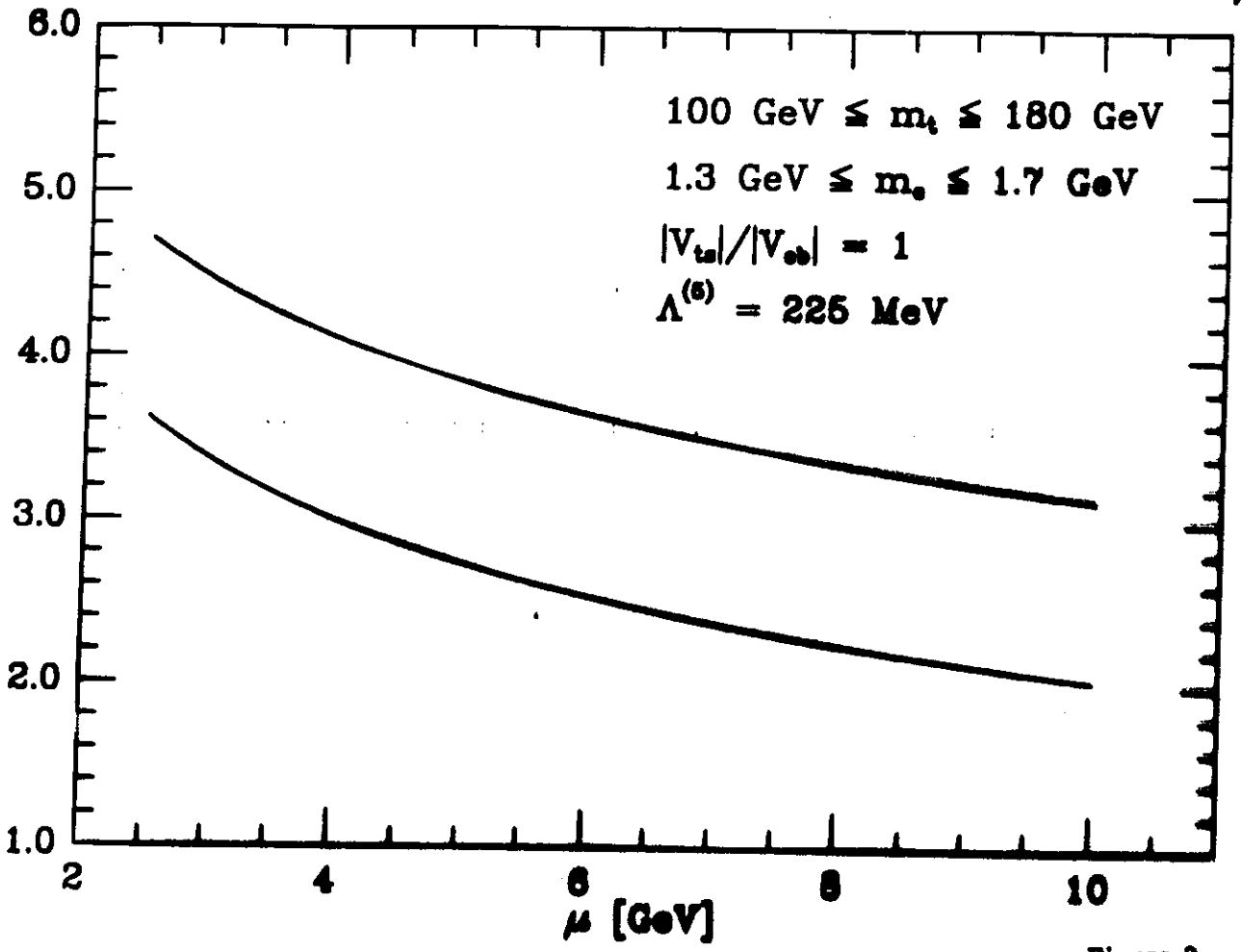

Figure 3

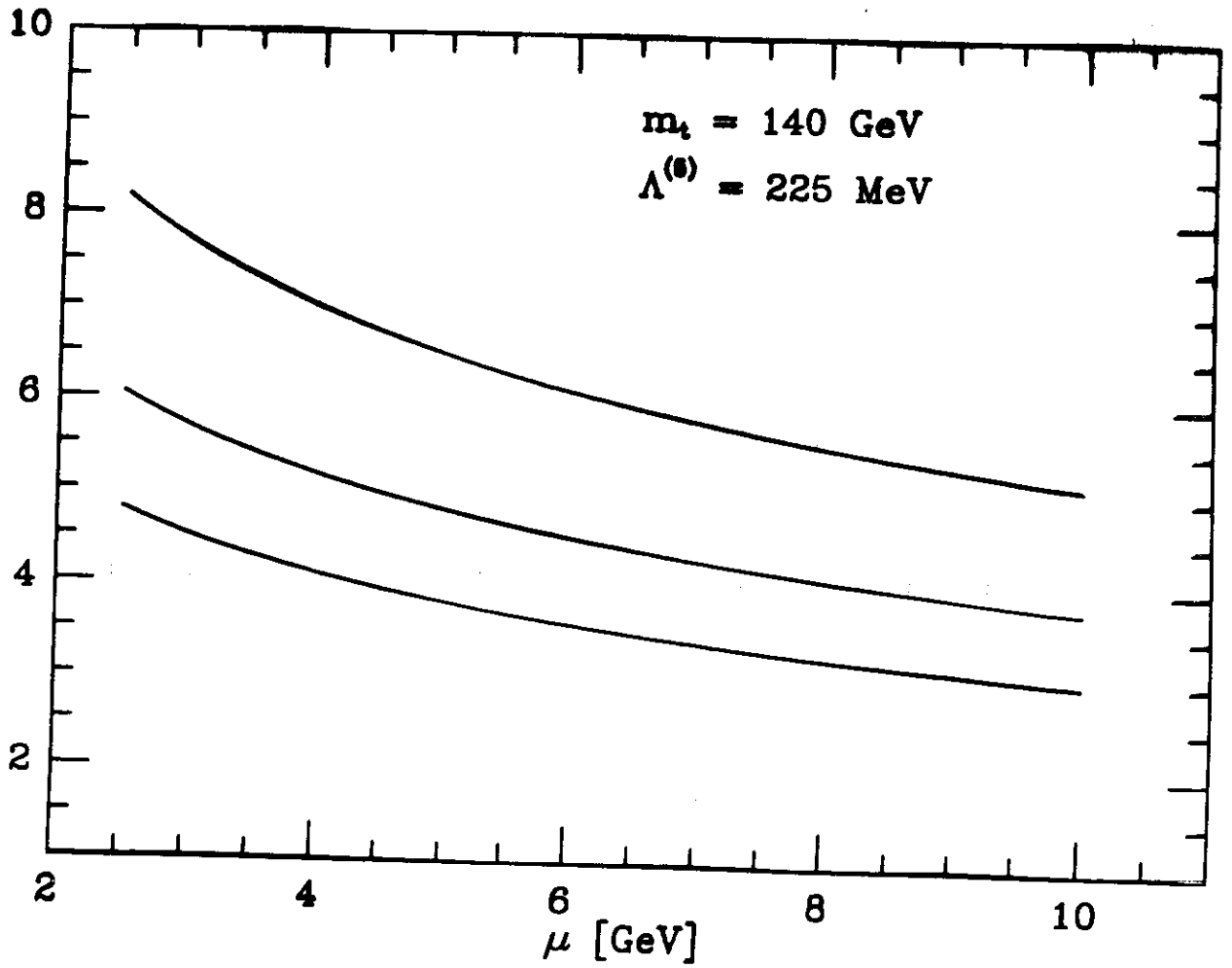

Grunb, A.A.

Figure 4

$b \to \gamma s$ INCLUSIVE RESULTS (CLEO)

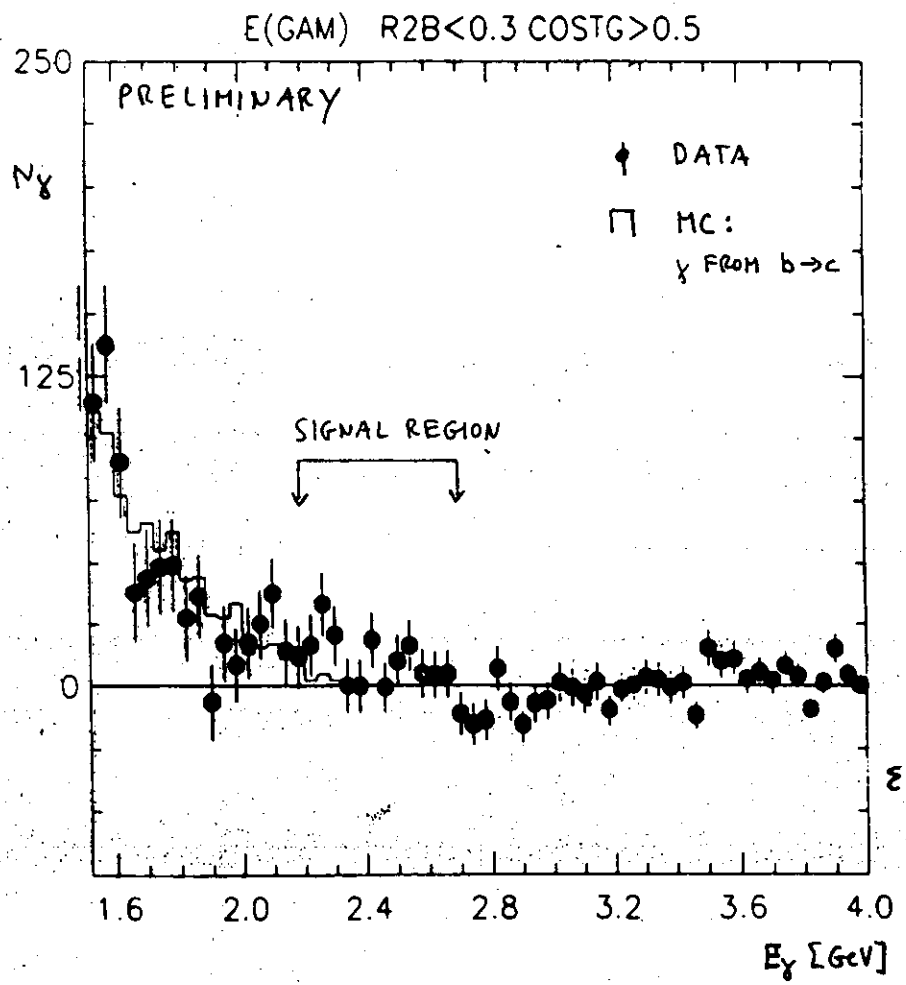

- OBSERVE $N_\gamma = 116 \pm 55$ PHOTONS IN $2.2 \le E_\gamma \le 2.7$
- OBSERVE $N_\gamma = 20 \pm 52$ PHOTONS IN CONTROL REGION OF CONTINUUM SUBTRACTION: $2.8 \le E_\gamma \le 4.0$ GeV

$\therefore$ $B(b \to s\gamma) < 9 \times 10^{-4}$ @ 90% CL

$f = (4.0 \pm 2.0) \times 10^{-4}$

$M_{K\pi\gamma}$ VS $M_{K\pi}$

- $\Delta E = E_{\gamma K\pi} - E_{beam} < 100$ MeV
- $|\cos\theta_{T\gamma}| < 0.7$

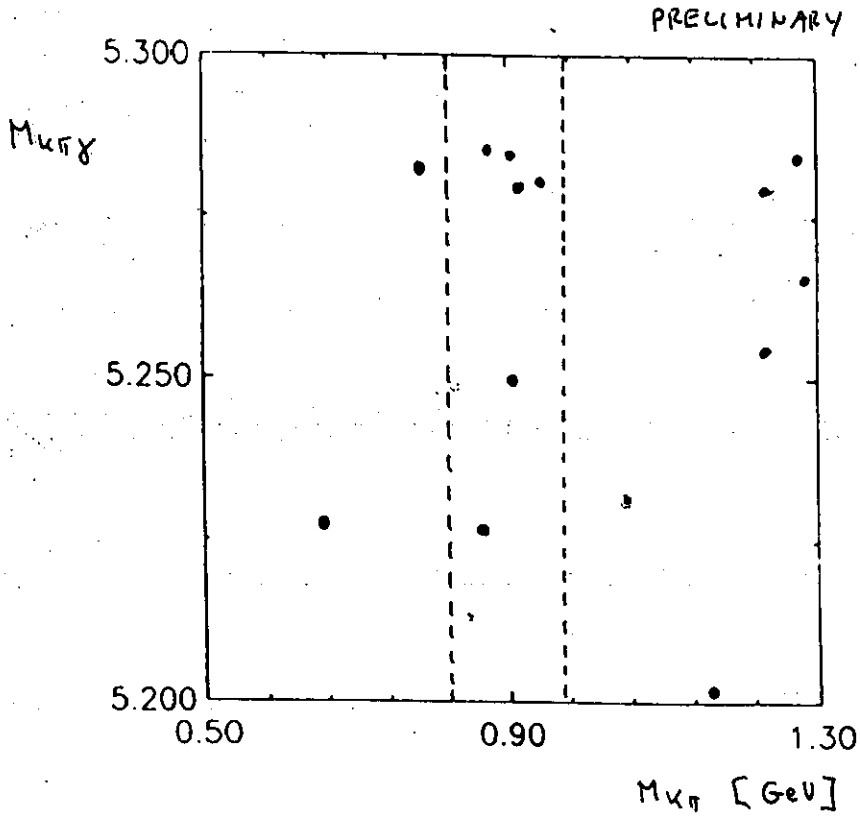

$b \to s\gamma$ EXCLUSIVE RESULTS (CLEO)

(PRELIMINARY)

Preliminary Upper Limits on Exclusive $K^*\gamma$ Modes

Decay mode	Eff(%)	BR ($\times 10^{-4}$) (90% C.L.) (Preliminary)
$\bar{B}^0 \to \bar{K}^{*0}(892)\gamma$	18	0.95 •
$B^- \to K^{*-}(892)\gamma$	5.2	3.7
$\bar{B}^0 \to \bar{K}_1^0(1270)\gamma$	3.6	5.5
$B^- \to K_1^-(1270)\gamma$	2.9	11
$\bar{B}^0 \to \bar{K}_1^0(1400)\gamma$	8.0	5.4
$B^- \to K_1^-(1400)\gamma$	11	4.8
$\bar{B}^0 \to \bar{K}_2^{*0}(1430)\gamma$	8.6	1.3
$B^- \to K_2^{*-}(1430)\gamma$	2.2	3.7
$\bar{B}^0 \to \bar{K}_3^{*0}(1780)\gamma$	3.6	7.6
$B^- \to K_3^{*-}(1780)\gamma$	2.8	14

• OBSERVE 4 EVENTS NEAR B-MASS

BACKGROUND $\simeq$ 1 EVENT

$\Rightarrow$ $\mathcal{B}(\bar{B}^0 \to \gamma K^*(890)) = (4.6 \pm 3.1) \times 10^{-5}$

3 FCNC B-DECAYS INVOLVING DILEPTONS

$b \to s\, \ell^+\ell^-$, $d\,\ell^+\ell^-$

$b \to s\, \nu\bar{\nu}$, $d\,\nu\bar{\nu}$

In this section

Wilson coefficients are, however, included in presenting the rates and distributions being discussed.

In the approximation of keeping only dimension-6 operators, the appropriate basis for the FCNC B-decays involving dileptons consists of twelve operators and the effective Hamiltonian may be written as

$$\mathcal{H}_{eff}(b \to s + \ell^+\ell^- \ (\ell = e, \mu)) = -\frac{4G_F}{\sqrt{2}}\lambda_t \sum_{j=1}^{12} \tilde{C}_j(\mu)\tilde{O}_j(\mu) \qquad (56)$$

Detailed considerations, however, show that the coefficients of some of the operators and their mixing with the remaining ones are small and the basis may be truncated. The operators of interest in the present context are, $\tilde{O}_1, \tilde{O}_2, \tilde{O}_7, \tilde{O}_8$ and $\tilde{O}_9$. The first three in this list were given in the previous section while discussing the decays $b \to s + \gamma + g$. Since the operators $\tilde{O}_j$ are used to calculate the matrix elements for the transition $b \to s$+(virtual) photon, we have to take a one loop matrix element of the operators $\tilde{O}_1, \tilde{O}_2$, and $\tilde{O}_7$. The remaining operators are defined below:

$$\tilde{O}_8 = \frac{\alpha}{4\pi}(\bar{s}\gamma_\mu L b)(\bar{\ell}\gamma_\mu \ell) \qquad (57)$$

$$\tilde{O}_9 = \frac{\alpha}{4\pi}(\bar{s}\gamma_\mu L b)(\bar{\ell}\gamma_\mu\gamma_5 \ell) \qquad (58)$$

and the Wilson coefficients are [35,34]

$$C_9(m_b) = C_9(M_W) + \frac{4\pi}{\alpha_s(M_W)}\left[\frac{4}{33}\left(1 - \eta^{-11/23}\right) - \frac{8}{87}\left(1 - \eta^{-20/23}\right)\right] \qquad (59)$$

$$C_8(m_b) = C_8(M_W) \qquad (60)$$

where we have dropped the tilde on the coefficients $\tilde{C}_i$ for ease of writing. To avoid possible mix-up in the notation, we point out that the operator $\tilde{O}_8$ in the effective Hamiltonian here and the operator $\hat{O}_8$ in the corresponding Hamiltonian for $b \to s + \gamma + g$ are different operators, hence also the Wilson coefficients C_8 in the two cases are different. Again, the large logarithms of the type $\ln(M_W^2/m_b^2)$ are included in the Wilson coefficients and not in the matrix elements of the operators.

The coefficients $C_9(m_W)$ and $C_8(m_W)$ appearing above can be written in terms of these functions B, C and D, following [34,35].

$$C_9(M_W) = \frac{1}{\sin^2\theta_W}B(x) + \frac{-1 + 4\sin^2\theta_W}{\sin^2\theta_W}C(x) + D(x) + \frac{4}{9} \qquad (61)$$

$$C_8(M_W) = \frac{-1}{\sin^2\theta_W}B(x) + \frac{1}{\sin^2\theta_W}C(x) \qquad (62)$$

with

$$B(x) = \frac{1}{4}\left[\frac{x}{x-1} - \frac{x}{(x-1)^2}\ln x\right] \qquad (63)$$

$$C(x) = \frac{x}{4}\left[\frac{-x/2 + 3}{x-1} - \frac{3x/2 + 1}{(x-1)^2}\ln x\right] \qquad (64)$$

$$D(x) = \frac{x}{4}\left[\frac{x^3/36 - 25x^2/36}{} \quad \frac{x^4/6 - 5x^3/3 + 3x^2 - 16x/9 + 4/9}{}\ln x\right] \qquad (65)$$

lou et al., $b \to s \ell^+ \ell^-$

ominguez, Paver, Riazuddin; Grinstein et al.

eshpande, Trampetic; NP B 319 (1989) 271

Faus + Wyler;

ini et al.

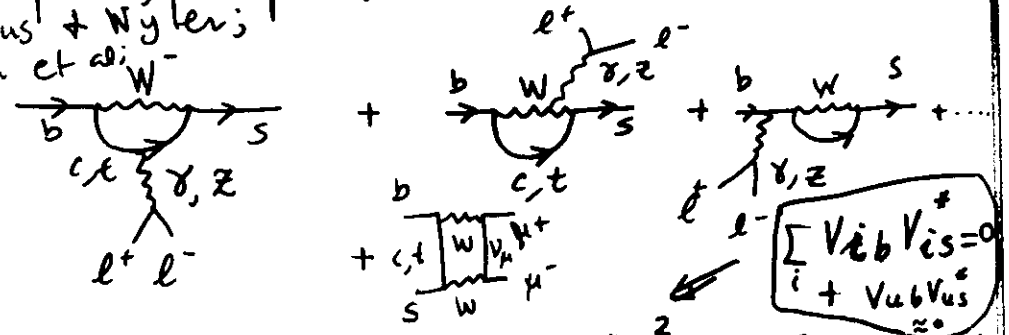

$$\mathcal{H}_{eff} = -\frac{4 G_F}{\sqrt{2}} |V_{tb} V_{ts}^*|^2 \sum_{j=1,2,7,8,9} C_j(\mu) O_j(\mu)$$

with

$$O_1 = (\bar{s}_{L\alpha} \gamma_\mu b_{L\alpha})(\bar{c}_{L\beta} \gamma^\mu c_{L\beta})$$

$$O_2 = (\bar{s}_{L\alpha} \gamma_\mu b_{L\beta})(\bar{c}_{L\beta} \gamma^\mu c_{L\alpha})$$

$$O_7 = \left(\frac{e^2}{16\pi^2}\right) m_b (\bar{s}_{L\alpha} \sigma^{\mu\nu} b_{R\alpha}) F_{\mu\nu}$$

$$O_8 = \left(\frac{e^2}{16\pi^2}\right)(\bar{s}_{L\alpha} \gamma_\mu b_{L\alpha}) \bar{\ell} \gamma^\mu \ell$$

$$O_9 = \left(\frac{e^2}{16\pi^2}\right)(\bar{s}_{L\alpha} \gamma_\mu b_{L\alpha}) \bar{\ell} \gamma^\mu \gamma^5 \ell$$

- $O_3 \cdots O_6$ same as for $\mathcal{H}_{eff}(b \to s\gamma)$, $C_{3,\ldots,6}$ Coeff. induced by mixing; small
- Also an operator O_{10} present [but not in $O(\alpha_s/\pi)$]

The matrix-element for the process of interest can be written as:

$$\mathcal{M}(b \to s + \ell^+\ell^-) = 2\sqrt{2} G_F \frac{\alpha}{\sin^2\theta_W} \lambda_t \frac{-1}{4\pi} \mathcal{M} \tag{66}$$

where we have again dropped the small terms due to the intermediate u-quark, and have used the CKM unitarity constraint to relate $\lambda_c \equiv V_{cb}V_{cs}^*$ to λ_t. The reduced matrix element $\mathcal{M}$ can be shown to be:

$$\mathcal{M} = C_A\, s_L \gamma_\mu b_L\, \bar{\ell}_L \gamma^\mu \ell_L + C_B\, s_L \gamma_\mu b_L\, \bar{\ell}_R \gamma^\mu \ell_R + 2\sin^2\theta_W C_7(\mu) \bar{s} i\sigma_{\mu\nu} q^\nu / q^2 (m_s L + m_b R) b\, \bar{\ell} \gamma_\mu \ell \tag{67}$$

As pointed out earlier, one has to calculate both the long- and short-distance contribution to $\mathcal{M}$. We concentrate first on the short distance piece and give the long distance contribution later. The functions C_A, C_B are given by:

$$C_A = \sin^2\theta_W(-C_8(m_b) + C_9(m_b) - (3C_1(m_b) + C_2(m_b))g(m_s/m_b, q^2)) \tag{68}$$

$$C_B = \sin^2\theta_W(-C_8(m_b) - C_9(m_b) - (3C_1(m_b) + C_2(m_b))g(m_s/m_b, q^2)) \tag{69}$$

and the function $g(m_s/m_b, q^2)$ arises from the one-loop matrix element of the four-quark operators [34,35]:

$$g(m_s/m_b, y) = -\left\{\frac{4}{9}\ln\left(\frac{m_c^2}{m_b^2}\right) - \frac{8}{27} - \frac{16}{9}\frac{m_c^2}{y} + \frac{2}{9}\sqrt{\left|1 - \frac{4m_c^2}{y}\right|}\left(2 + \frac{4m_c^2}{y}\right) R(y)\right\} \tag{70}$$

with

$$R(y) = \ln\left|\frac{1 + \sqrt{1 - \frac{4m_c^2}{y}}}{1 - \sqrt{1 - \frac{4m_c^2}{y}}}\right| + i\pi \quad \text{for } y > 4m_c^2 \tag{71}$$

$$R(y) = 2\arctan\left(\frac{1}{\sqrt{1 - \frac{4m_c^2}{y}}}\right) \quad \text{for } y < 4m_c^2 \tag{72}$$

The invariant dilepton mass distribution in the inclusive decays can now be calculated easily with the help of the matrix elements, given above. For the inclusive decay rate contribution from the short-distance piece, one estimates:

$$\boxed{BR(B \to X_s + e^+e^-) = (1-2) \times 10^{-6}}$$

and

$$\boxed{BR(B \to X_s + \mu^+\mu^-) = (6-8) \times 10^{-6}} \tag{73}$$

for the top quark mass range, 100 GeV $< m_t <$ 200 GeV. These estimates are to be contrasted with the recent upper limit for the (averaged) B-meson branching ratio from the UA1 collaboration: $BR(B \to X + \mu^+\mu^-) = 5 \times 10^{-6}$ [59], indicating that the present experimental sensitivity is an order of magnitude away in this channel. The branching ratios for the Cabibbo-suppressed FCNC decays $b \to d + \ell^+\ell^-$ ($\ell = e, \mu$) can be obtained by scaling the corresponding $b \to s + \ell^+\ell^-$ ($\ell = e, \mu$) rates by the CKM factor $(|V_{td}|/|V_{ts}|)^2$. The relative rates $BR(B \to X_d + \ell^+\ell^-)/BR(B \to X_s + \ell^+\ell^-)$ are independent of m_t and their eventual

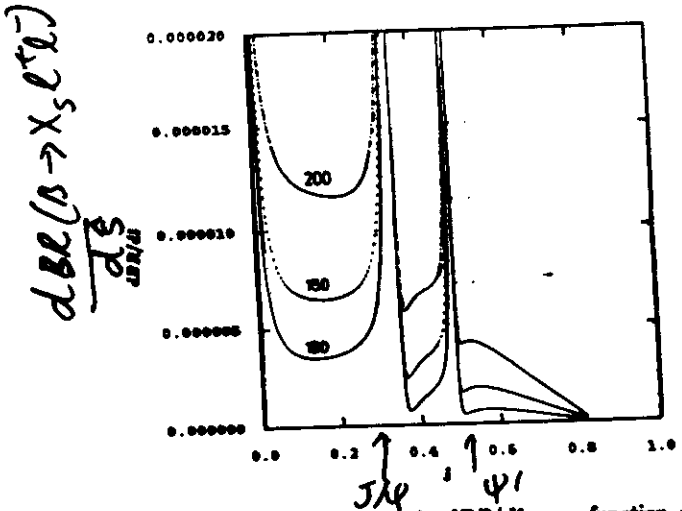

$\hat{s} = \frac{m_{\ell^+\ell^-}^2}{m_B^2}$

Figure 9: The differential branching ratio $dBR/d\hat{s}$ as a function of the scaled invariant dilepton mass $\hat{s} = s/m_b^2$ in the decay $b \to s + \ell^+\ell^-$ ($\ell = e, \mu$). Assumed top quark mass values are indicated on the curves (from ref. [40]).

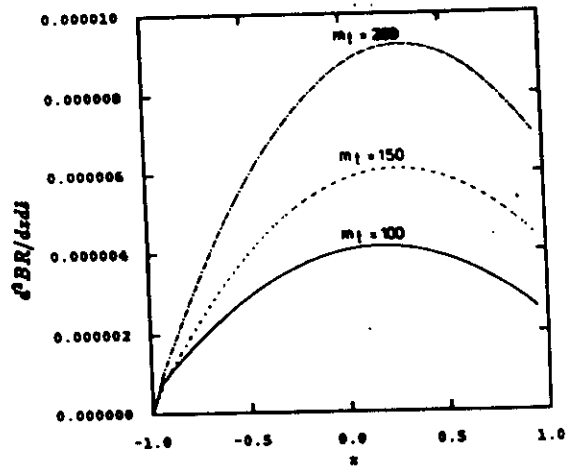

Figure 10: The angular distribution $d^2BR/dxd\hat{s}$ in the decay $b \to s + \ell^+\ell^-$ ($\ell = e, \mu$), for a fixed value of the scaled dilepton invariant mass $\hat{s} = 0.3$. The assumed top quark mass values $m_t = 100,\ 150,\ 200\ GeV$ are indicated on the curves. (from ref. [40]).

Ali, Mannel, Morozumi

S.D. + L.D.

$b \to s\ell^+\ell^-$

J/ψ ψ'

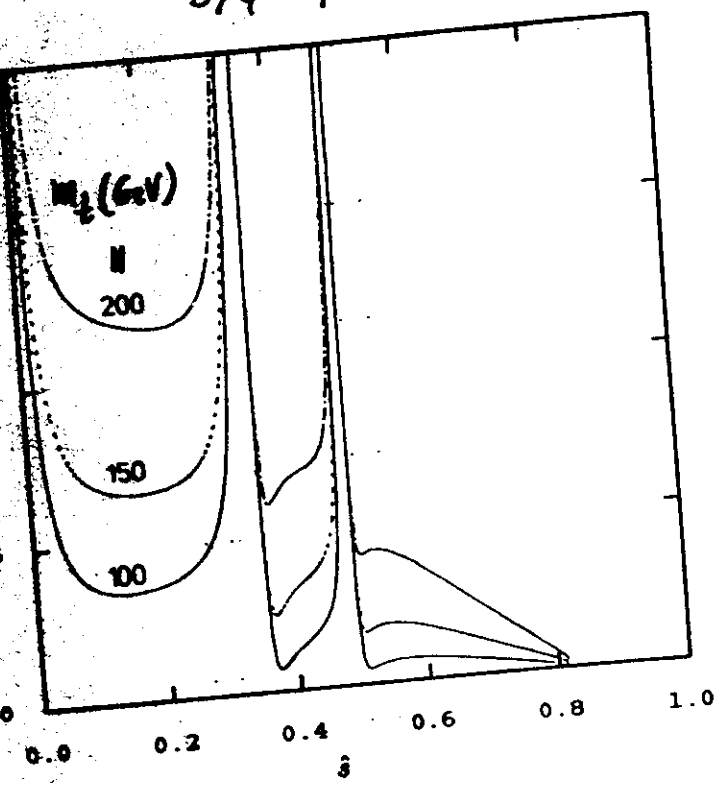

Figure (1)

Invariant dilepton mass dish.

$\frac{dBR}{d\hat{s}}(b \to s\ell^+\ell^-)$

- Interference is +ve
- S.D. Contr. is sensitive to m_t

Ali, Mannel, Morozumi

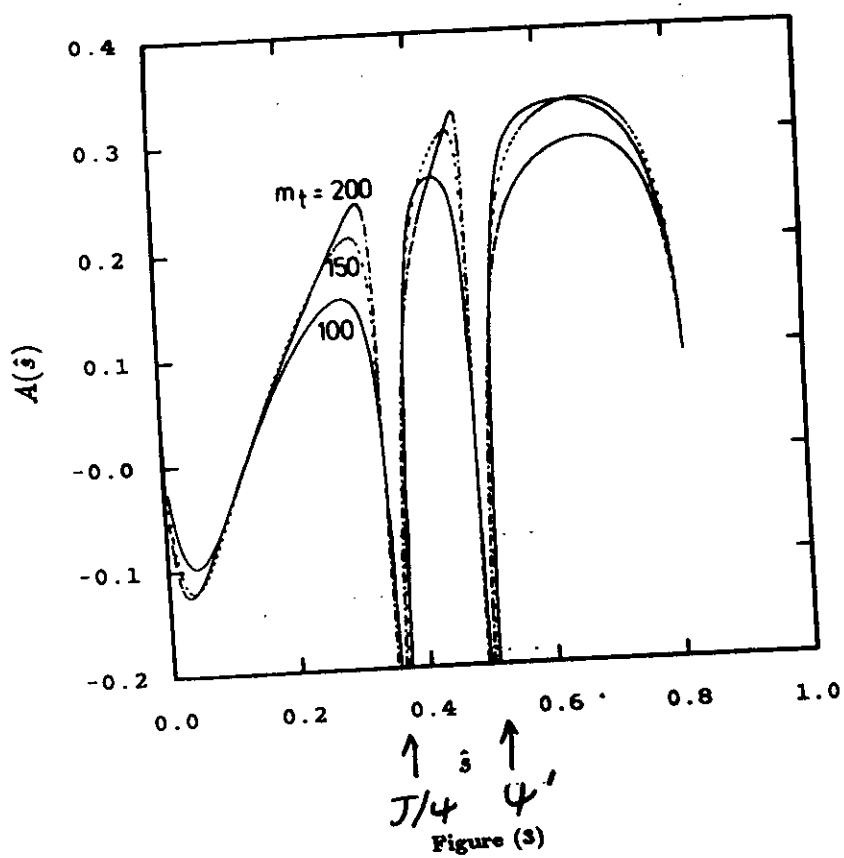

Figure (3)

Forward - Backward Asymmetry in $b \to s + \ell^+\ell^-$

$$A(\hat{s}) = \frac{\int_0^1 dz \frac{d^2BR}{d\hat{s}dz} - \int_{-1}^{0} dz \frac{d^2BR}{d\hat{s}dz}}{\Gamma \quad + \int}$$

UA1 Collaboration ('91)

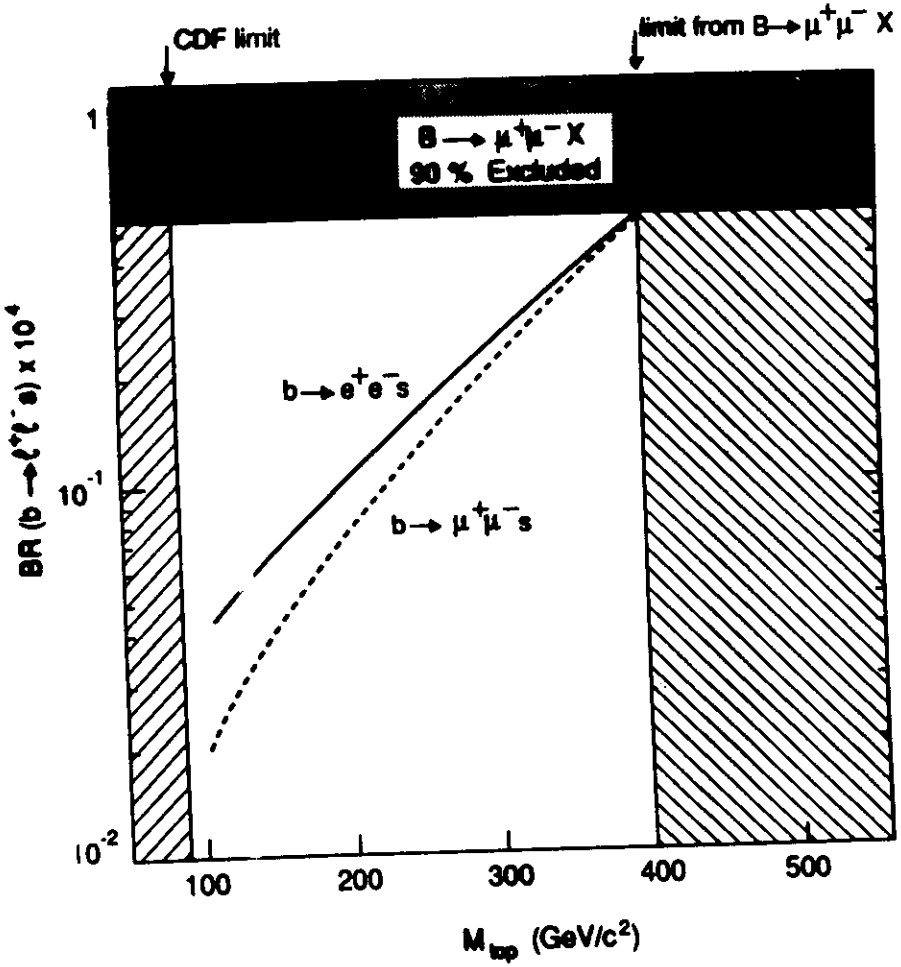

FIG. 6

$$BR(B^0 \to \mu^+\mu^-) < 8.3 \times 10^{-6}$$
$$BR(B^0 \to \mu^+\mu^- X) < 5.0 \times 10^{-5}$$

$b \to s \nu\bar{\nu}$

$$\mathcal{H}_{eff} = -\frac{8 G_F}{\sqrt{2}} V_{tb} V_{ts}^* C_q(m_W) \left(\frac{\alpha}{4\pi}\right) (\bar{s} \gamma_\mu L b)(\bar{\nu} \gamma_\mu L \nu)$$

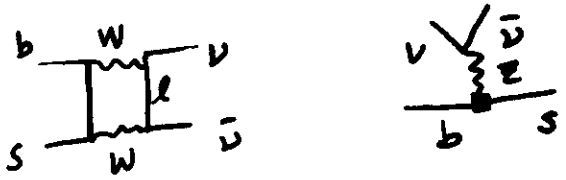

no QCD Corrections: $C_q(m_W) \simeq C_q(m_W)$

$$C_q(x) = \frac{1}{\sin^2\theta_W}\left[\frac{1}{8}x + \frac{3x(x-2)}{8(x-1)^2}\ln x + \frac{3}{8}\frac{x}{x-1}\right]$$

$\Rightarrow$ $BR(b \to s\nu\bar{\nu}) = 4 \times 10^{-5}$ for $m_t = 150$ GeV

Difficult Expt. !

except perhaps for High Luminosity LEP Expts.

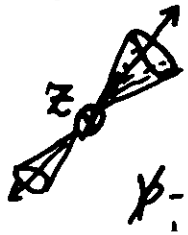

Signature: Highly $\not{p}$-imbalanced b-jets

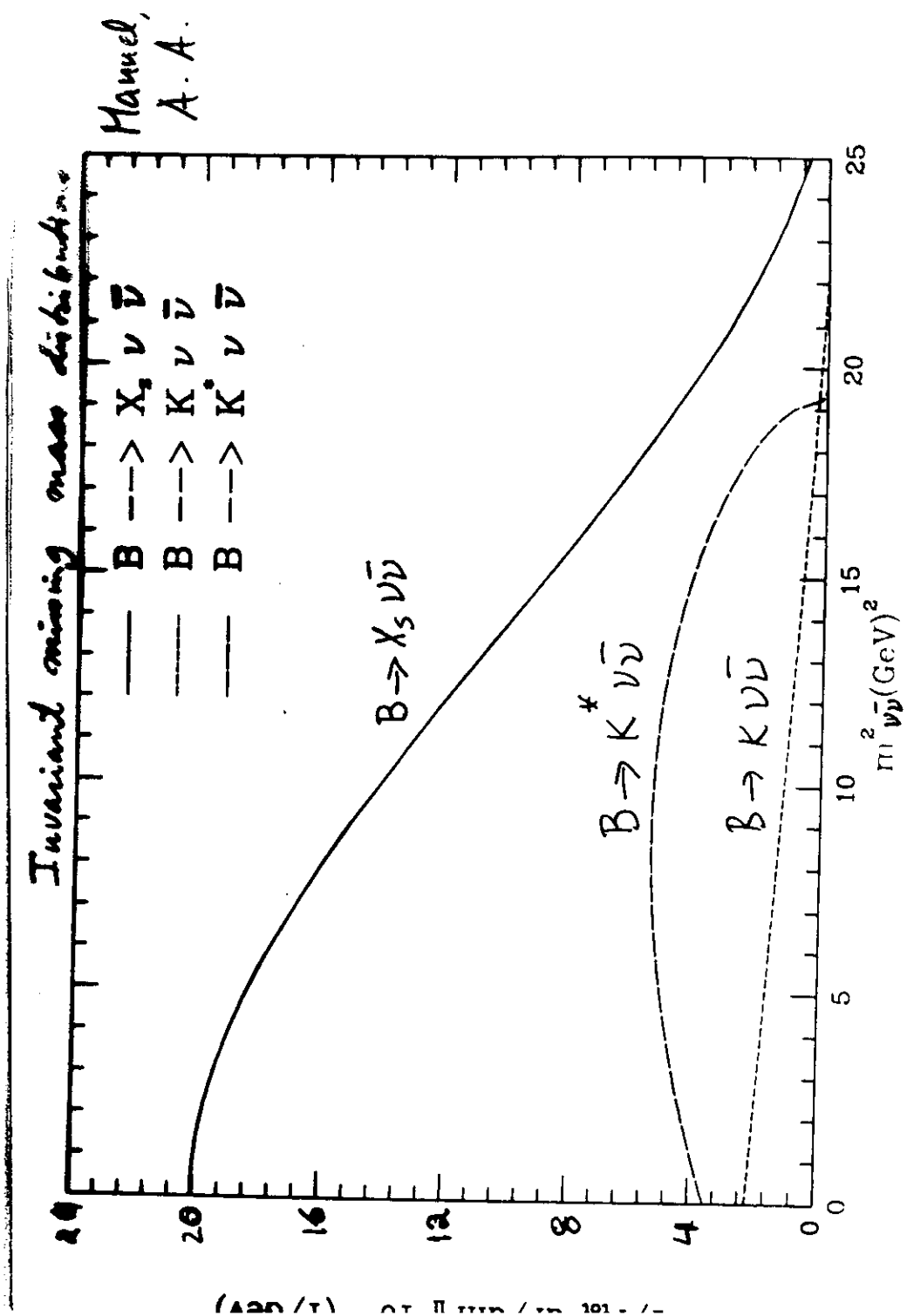

OVERVIEW and OULOOK

Decay Modes	Br	Experimental Upper Limits (90 % C.L.)
$(B_d, B_u) \to X_s\gamma$	4.2×10^{-4}	8.4×10^{-4} [redacted]
$(B_d, B_u) \to K^*\gamma$	$(4.0 - 7.0) \times 10^{-5}$	6.92×10^{-4} [redacted]
$(B_d, B_u) \to X_d\gamma$	$(0.5 - 3.0) \times 10^{-5}$	–
$(B_d, B_u) \to \rho + \gamma$	$(1.0 - 3.0) \times 10^{-5}$	–
$(B_d, B_u) \to X_s e^+e^-$	1.2×10^{-5}	–
$(B_d, B_u) \to X_s \mu^+\mu^-$	6.7×10^{-6}	5.0×10^{-5} [UA1] [50]
$(B_d, B_u) \to K e^+e^-$	4.4×10^{-7}	5.0×10^{-5} [PDG] [13]
$(B_d, B_u) \to K \mu^+\mu^-$	4.4×10^{-7}	1.5×10^{-4} [PDG] [13]
$(B_d, B_u) \to K^* e^+e^-$	3.7×10^{-6}	–
$(B_d, B_u) \to K^* \mu^+\mu^-$	2.3×10^{-6}	2.3×10^{-4} [UA1] [50]
$(B_d, B_u) \to X_s \nu\bar{\nu}$	6.6×10^{-5}	–
$(B_d, B_u) \to K \nu\bar{\nu}$	5.2×10^{-6}	–
$(B_d, B_u) \to K^* \nu\bar{\nu}$	2.0×10^{-5}	–
$B_s \to \gamma\gamma$	2.0×10^{-6}	–
$B_s \to \tau^+\tau^-$	1.8×10^{-7}	–
$B_s \to \mu^+\mu^-$	8.3×10^{-10}	–
$B_s \to e^+e^-$	2.0×10^{-14}	–

Table 9: Estimates of the branching fractions for FCNC B-decays in the Standard Model for $m_t = 150\ GeV$ and $f_B = 200\ MeV$. Note that the CKM-suppressed decays, given in row 3 and 4, depend on $|V_{td}|$, and the numbers correspond to $|V_{td}| = 0.007$. Experimental upper limits are also listed.

Present bounds + measurements

Selected Rare K Decay Searches[1] (other than 787)		
Lab/Experiment	Result	Notes
BNL 791	$B(K_L \to \mu^+\mu^-) = (7.1 \pm .4 \pm .4) \times 10^{-9}$	2,3
KEK 137	$B(K_L \to \mu^+\mu^-) = (8.2 \pm .8 \pm .7) \times 10^{-9}$	2
BNL 791	$B(K_L \to \mu^\pm e^\mp) < 8.4 \times 10^{-11}$	2
KEK 137	$B(K_L \to \mu^\pm e^\mp) < 4.3 \times 10^{-10}$	2
BNL 791	$B(K_L \to e^+e^-) < 1.1 \times 10^{-10}$	2
KEK 137	$B(K_L \to e^+e^-) < 5.6 \times 10^{-10}$	2
BNL 777	$B(K^+ \to \pi^+\mu^+e^-) < 2.1 \times 10^{-10}$	
BNL 845	$B(K_L \to \pi^0 e^+e^-) < 5.5 \times 10^{-9}$	
FNAL 731	$B(K_L \to \pi^0 e^+e^-) < 7.5 \times 10^{-9}$	
CERN NA31	$B(K_L \to \pi^0\gamma\gamma) = (2.1 \pm .6) \times 10^{-6}$	4
FNAL 731	$B(K_L \to \pi^0\gamma\gamma) = (1.86 \pm .60 \pm .65) \times 10^{-6}$	4

Notes:

1) Upper limits are 90% C.L.
2) More data to be analysed
3) Average of '88 & '89 data.
4) Sensitive to $m_{\gamma\gamma} > 280$ MeV/c^2

$B(K^+ \to \pi^+ \nu\bar{\nu}) < 3.4 \times 10^{-9}$ [PDG]

$B(K^+ \to \pi^+ \nu\bar{\nu}) < 5 \times 10^{-9}$ [E787 @ BNL]

(Buras et al)

SM Predictions for

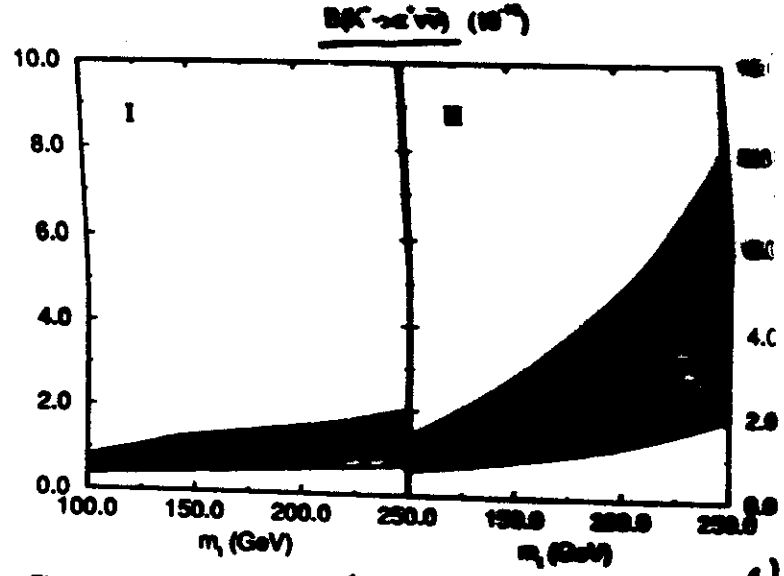

Fig. 16: The decay $K^+ \to \pi^+ \nu\bar{\nu}$ (m_c = 1.4 GeV assumed)

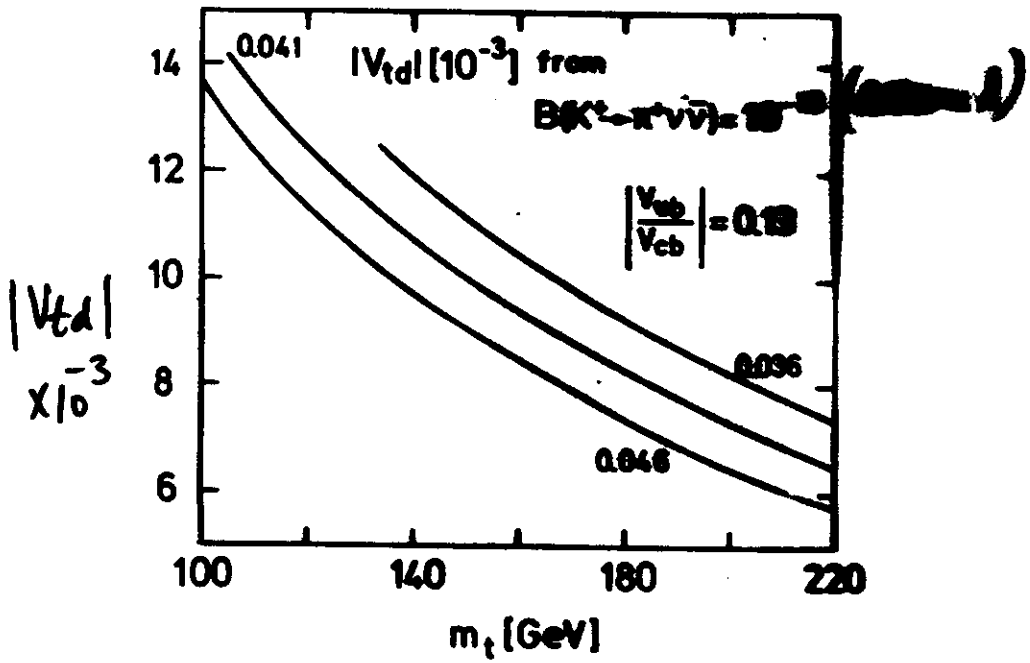

(Buras et al.)

SM Predictions for

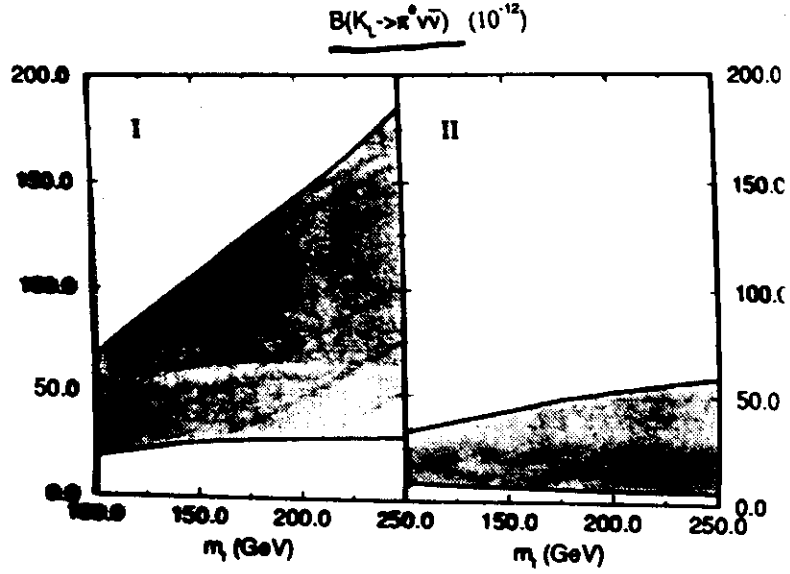

Fig. 18: The decay $K_L \to \pi^0 \nu\bar{\nu}$

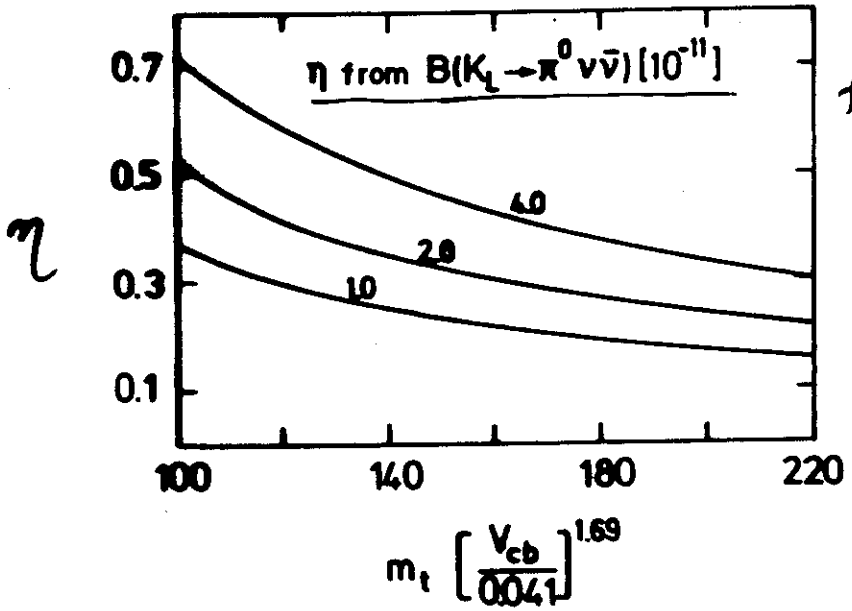

η from assumed value of $B(K_L \to \pi^0 \nu\bar{\nu})$

SM predictions for (Buras et al)

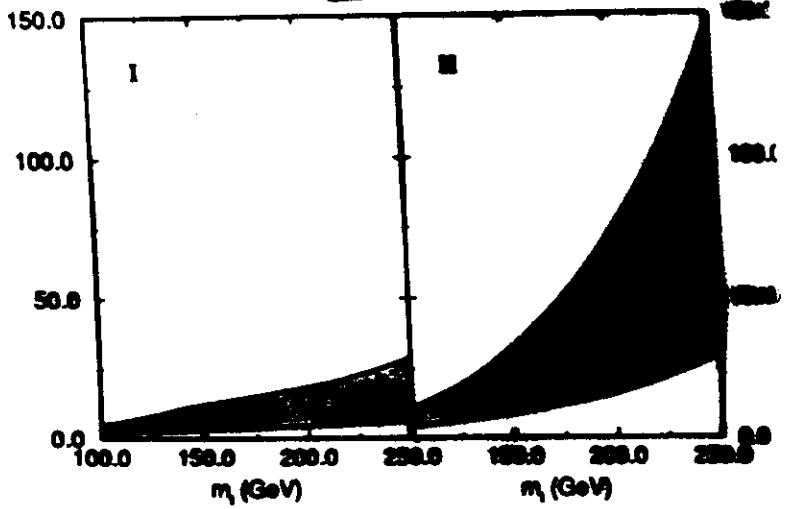

Fig. 31: The decay $K_L \to \mu^+\mu^-$

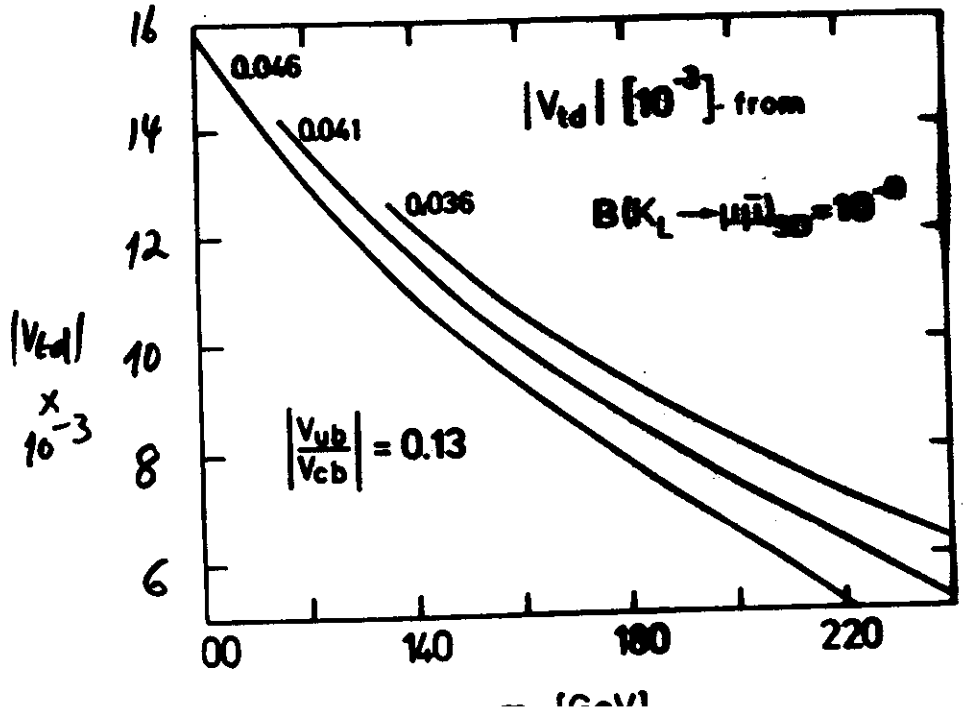

CP Violation in K-Decays

ϵ'/ϵ

Theory: $\simeq 0$ Compatible with SM predictions for $m_t = \mathcal{O}(200\,\text{GeV})$
Dependence on Matrix Element of penguin Operatn

Expt: PDG ('90)

$$\frac{\epsilon'}{\epsilon} = (2.2 \pm 1.1) \times 10^{-3}$$

However, disagreement between CERN & FNAL Exp

$K_L \to \pi^0 e^+ e^-$

$$K_L \simeq K_2 + \epsilon K_1$$

(K_2: CP odd) (K_1: CP even)

• 3 Contributions

1) CP Conserving: $K_2 \to \pi^0 \gamma\gamma \to \pi^0 e^+ e^-$

$BR(K_2 \to \pi^0 e^+ e^-) \simeq 10^{-14}$ [ChPT]

$\simeq 10^{-11}$ [Vector dominance Model

2) "Indirect" $\not CP$

$$K_1 \to \pi^0 \gamma_{Virt.} \to \pi^0 e^+ e^-$$

Estimate: $BR(K_L \to \pi^0 e^+ e^-)_{indirect} \simeq 0.58 \times 10^{-11}$

3) Direct $\not CP$

$$K_2 \to \pi^0 \gamma_{Vir} \to \pi^0 e^+ e^-$$

Estimate: $\boxed{BR(K_L \to \pi^0 e^+ e^-)_{direct} \sim 8 (10^{-11})}$

[Interplay of electromag. + Weak penguins + WW Box cont.]

Present Limit: $BR(K_L \to \pi^0 e^+ e^-) < 5.5 \times 10^{-9}$ [BNL]

ϕ - Factory (Frascati) $\Rightarrow$ $O(10^{-11})$ Sensitivity

[BNL, KEK, CERN, FNAL]

Rare K-decay Searches

Bad News: $K_L \to e^+ e^- \gamma\gamma$

5 events $\Rightarrow$ $BR(K_L \to e^+ e^- \gamma\gamma) \sim 5.8 \times 10^{-7}$ [...cut]

Dib, Dunietz, Gilman.

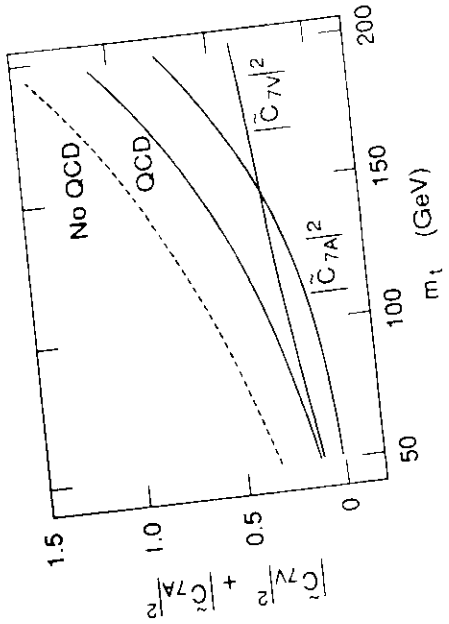

Fig. 10

$$BR(K_L \to \pi^0 e^+ e^-)_{direct} \simeq 10^{-5} (s_2 s_3 s\delta)^2 \left[|\tilde{C}_7|^2 + |\tilde{C}_{7A}|^2 \right]$$

$$\simeq 10^{-11} \left[|\tilde{C}_7|^2 + |\tilde{C}_{7A}|^2 \right]$$

$K_L \to \pi^0 e^+ e^-$

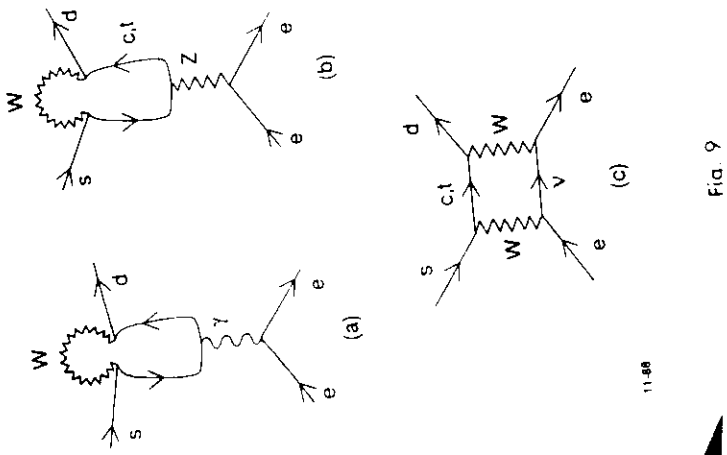

Fig. 9

BNL 845 - BNL / YALE

(Morse, Schmidt, Adair et al

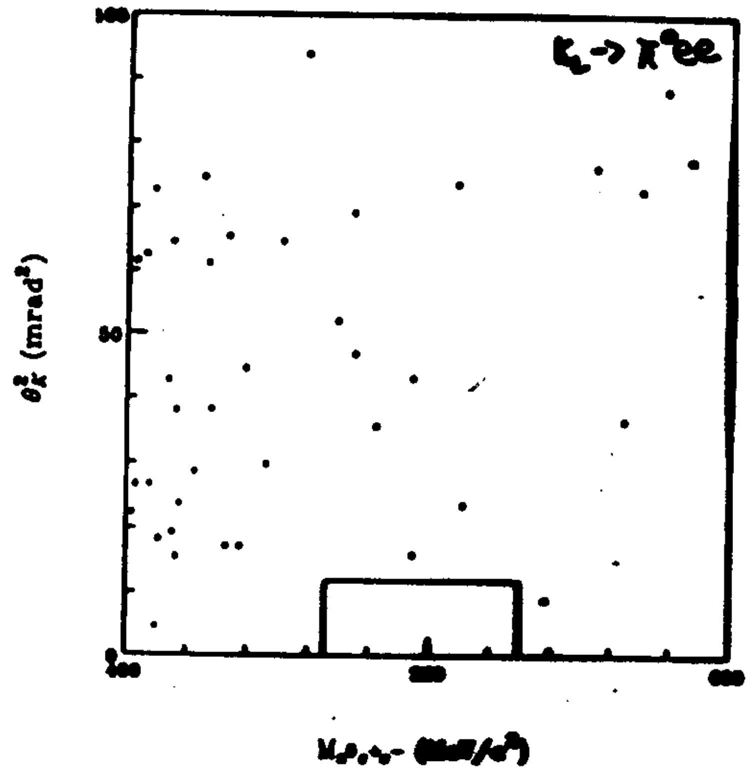

$BR(K_L \to \pi^0 e^+ e^-) < 5.5 \times 10^{-9}$ (90%)

KEK Expt is running (KEK 162)
FNAL 799 is now approved.
goal: $10^{-10} - 10^{-11}$

Rare t-decays

$t \to c V$, $V = \gamma, Z, g, H$

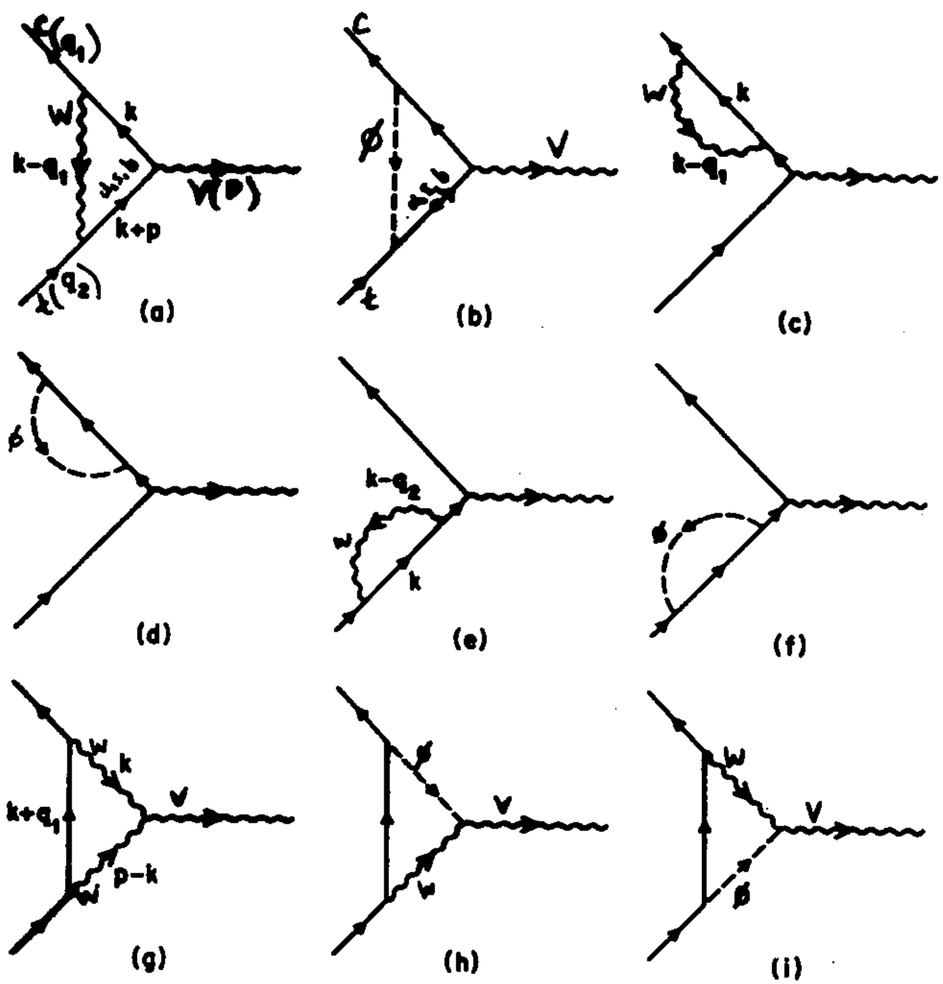

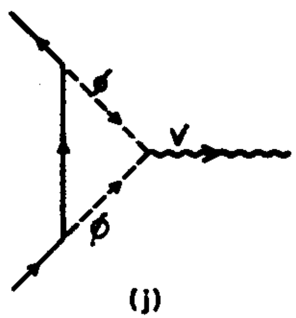

Standard Model Feynman Diagrams

't Hooft - Feynman Gauge
(R_ξ , $\xi = 1$)

Deshpande, Margolis, Trottier

Virtual gluon mode is enhanced over on-shell gluon due to large logs in the loop quark masses

- further enhancements in anomalous threshold region

Define $B(t \to cX) = \frac{\Gamma(t \to cX)}{\Gamma(t \to bW)}$

Eilam, Hew So

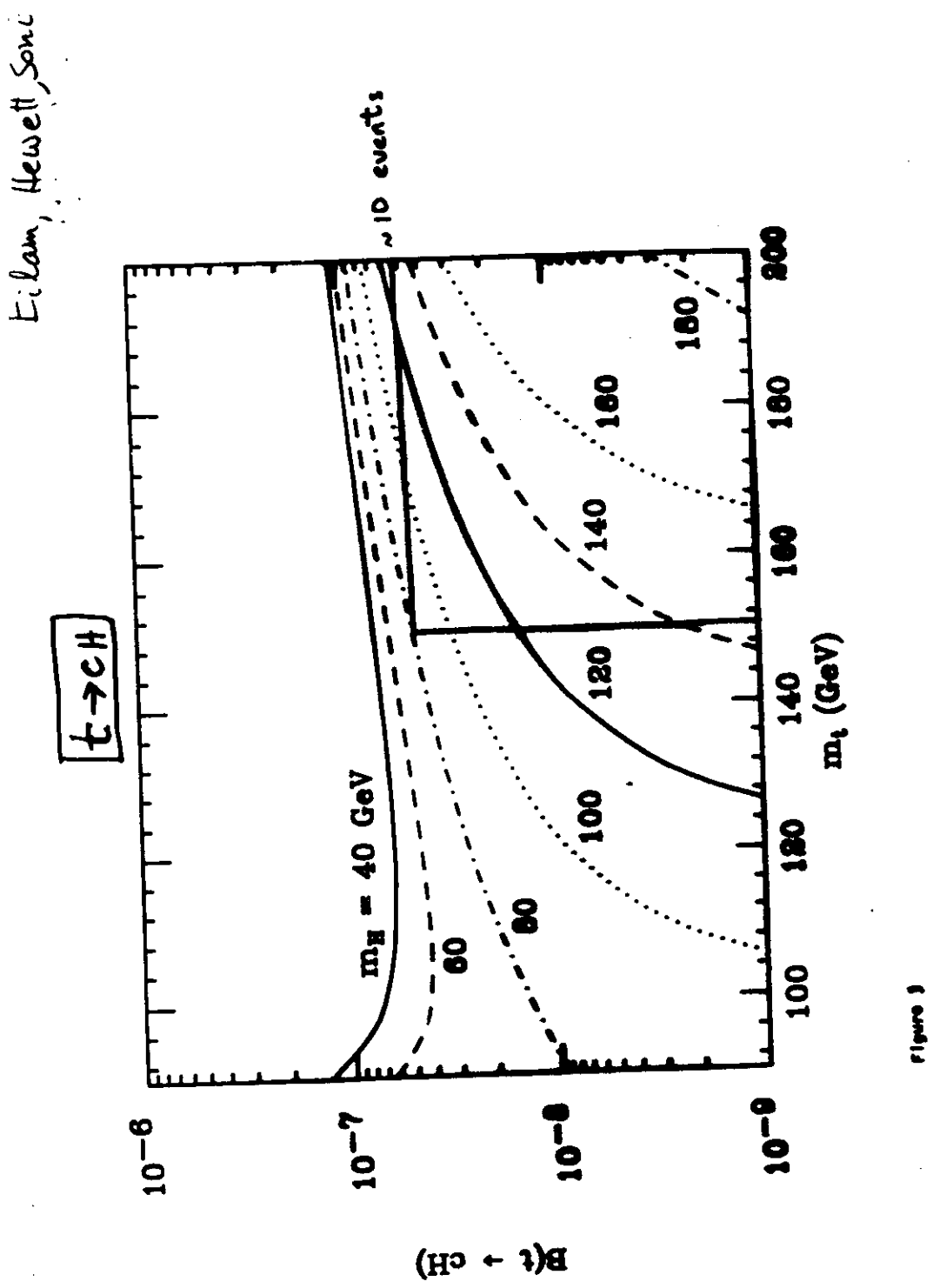

Figure 3

Rare t-decay Rates

($m_t = 150$ GeV) Eilam, Hewett, Soni; Deshpande et al.; ...

$BR(t \to cH)$	5×10^{-8}	$m_H = 80$ GeV
	1×10^{-8}	$m_H = 120$ GeV
$BR(t \to cg^* \to \bar{c} q\bar{q})$	2×10^{-10}	
$BR(t \to cg)$	1×10^{-10}	
$BR(t \to c\gamma)$	1×10^{-12}	
$BR(t \to cZ)$	3×10^{-13}	

- Rare t-decays out of experimental reach if SM governs FCNC interactions
- good window to search for ... Physics